UPPSALA
UNIVERSITET

UPTEC F12 022
Examensarbete 30 hp
Juli 2012

Modeling of Ion Injection in Oil-Pressboard Insulation Systems

Christian Sonehag

UPPSALA
UNIVERSITET

Teknisk- naturvetenskaplig fakultet
UTH-enheten

Besöksadress:
Ångströmlaboratoriet
Lägerhyddsvägen 1
Hus 4, Plan 0

Postadress:
Box 536
751 21 Uppsala

Telefon:
018 – 471 30 03

Telefax:
018 – 471 30 00

Hemsida:
http://www.teknat.uu.se/student

Abstract

Modeling of Ion Injection in Oil-Pressboard Insulation Systems

Christian Sonehag

To make a High Voltage Direct Current (HVDC) transmission more energy efficient, the voltage of the system has to be increased. To allow for that the components of the system must be constructed to handle the increases AC and DC stresses that this leads to. One key component in such a transmission is the HVDC converter transformer. The insulation system of the transformer usually consists of oil and oil-impregnated pressboard. Modeling of the electric DC field in the insulation system is currently done with the ion drift diffusion model, which takes into account the transport and generation of charges in the oil and the pressboard. The model is however lacking a description of how charges are being injected from the electrodes and the oil-pressboard interfaces. The task of this thesis work was to develop and implement a model for this which improves the result of the ion drift diffusion model.

A theoretical study of ion injection was first carried out and proceeding from this, a model for the ion injection was formulated. By using experimental data from 5 different test geometries, the injection model could be validated and appropriate parameter values of the model could be determined. By using COMSOL Multiphysics®, the ion drift diffusion model with the injection model could be simulated for the different test geometries.

The ion injection gave a substantial improvement of the ion drift diffusion model. The positive injection from electrodes into oil was found to be in the range 0.3-0.6 while the negative injection was 0.3 lower. Determination of the parameters for the injection from oil-pressboard interfaces proved to be difficult, but setting the parameters in the range 0.01-1 allowed for a good agreement with the experimental data. Here, a fit could be obtained for multiple assumptions about the set of active injection parameters.

Finally it is recommended that the investigation of the ion injection continues in order to further improve the model and more accurately determine the parameters of it. Suggestions on how this work could be carried out are given in the end.

Handledare: Olof Hjortstam
Ämnesgranskare: Shili Zhang
Examinator: Tomas Nyberg
ISSN: 1401-5757, UPTEC F12 022

Populärvetenskaplig Sammanfattning:

Den nu pågående omställningen till ett mer hållbart samhälle innebär ökade investeringar i förnyelsebara energikällor världen över. Vi ser till exempel en kraftig utbyggnad av vindkraftsparker och på många håll i världen byggs även vattenkraften ut. För att överföra den genererade elektriska energin till konsumenterna används ofta en högspänd likströmsöverföring. I ändarna på detta överföringssystem finns det transformatorer som omvandlar elen till och från den form som är bäst anpassad för överföringen. Dessa transformatorer måste designas så att de tål de elektriska påfrestningar som de utsätts för. För att ta fram en bra design måste de elektriska påfrestningarna kunna beräknas för olika testdesigner. Idag finns en fungerande modell för detta men den behöver utvidgas med en beskrivning av hur joner injiceras i systemet. Detta examensarbete har gått ut på att utveckla och utvärdera en modell för denna injektion.

Jämförelser mellan simuleringsresultat och experimentell data visade tydligt att den framtagna modellen förbättrar beräknandet av de elektriska påfrestningarna. Dock behöver detaljer i modellen genomarbetas ytterligare för att den ska bli fullständig nog för att kunna användas i verkligheten. När den väl blir mogen för det kommer den att kunna bidra till en transformatordesign som förutom att tåla högre elektriska påfrestningar också kommer vara både mindre och billigare.

TABLE OF CONTENTS

1 INTRODUCTION

One of the global challenges today is to meet the worlds growing need of energy. In the effort to achieve a sustainable society, the use of renewable energy sources is being intensified. Hydro power energy is generated at remote locations far away from the consumers. It is then important to be able to transfer bulk power over long distances with minimal losses. Offshore wind farms require cables to transfer the bulk power. The capacitance of these cables makes it problematic to use AC. The use of an Ultra High Voltage Direct Current (UHVDC) transmission would be optimal for these applications.

The UHVDC is making use of three important properties of resistive losses in electrical conduction. Firstly the losses in a transmission line decreases with increased voltage of the system. This is why it is sought to increase the voltage of the transmission lines. Secondly, since AC transmission suffers from the skin effect, DC is used instead of AC. The skin effect will distribute most of the current at the surface of the conductor leading to higher resistive losses. The third property of a DC transmission is that there is no reactive power giving rise to additional resistive losses.

Figure 1. Picture of an UHVDC transformer. Photo: ABB

The conversion from AC to UHVDC and back is very costly and this is why the DC transmission becomes favorable over long distances. To convert AC into HVDC, DC converters are used in conjunction with power transformers. One such converter transformer is presented in Figure 1. Typically a converter transformer has an insulation system consisting of a combination of mineral oil and solid cellulosic insulation in the form of pressboard and paper.

There is a desire to make the transformers as reliable and compact as possible. This is due to the increasing demand for higher voltages and power ratings and at the same time growing costs for the materials used in transformers. To allow for a more optimal design of the transformers the AC and DC stresses that a transformer is subjected to has to be better understood.

The AC field can already be calculated accurately since it is not dependent on the existence of free charges in the transformer insulation. This is not the case for the DC fields, which depends on the generation and transport of free charges in the oil and the pressboard. There exists a model called the ion drift diffusion model that correctly describes the DC field behavior in transformer oil [1]. The model is however lacking a good physical description of how charges are injected into the oil from the electrodes and oil-pressboard interfaces. This is the topic of this master thesis project.

Initially a model for the ion injection will be treated. The ion drift diffusion model will then be implemented in COMSOL Multiphysics® together with the model for the ion injection. This way the behavior of the charge injection model can be analyzed for different cases. This also allows the model to be validated against already attained experimental results for different test geometries.

In Section 2 the physical description of the ion drift diffusion model is presented together with the theory of ion injection. Thereafter different test geometries used for validation are presented in Section 3. How the implementation of the problem was done in COMSOL Multiphysics® is described in Section 4. The results of the simulations performed are presented in Section 5 and then discussed in Section 6. Finally some conclusions are drawn and some future work is suggested.

2 PHYSICAL DESCRIPTION

To model the DC electric behavior of a transformer insulation system, equations describing the charge generation and transport in the oil and the pressboard are established. Thereafter a model for ion injection from the electrodes and the oil-pressboard interfaces are presented. Finally the model for the ion injection is used to lay out boundary conditions between the oil and the pressboard as well as between the oil and the electrodes.

2.1 Ion Drift Diffusion Model

The transformer oil used in insulation systems mainly gets its electrical conductivity from the free ions that are dissolved in it. Ions in the oil exist partly as free ions and partly as ion pairs. The free ions can be recombined into ions pairs and the ion pairs can further be dissociated into free ions accordingly

$$A^+B^- \underset{k_R}{\overset{k_D}{\rightleftharpoons}} A^+ + B^- \tag{1}$$

Here k_D and k_R are the dissociation and recombination rate constants. The concentration of positive and negative ions will now be represented as p and n and the concentration of ion pairs as c. We can then describe the process of charge generation with the following rate equation

$$\frac{dp}{dt} = \frac{dn}{dt} = k_D c - k_R pn \tag{2}$$

Since the transformer oil can be considered a weak electrolyte [2] only a few of the ion pairs will be dissociated into ions. The concentration c of the ion pairs can therefore be considered as a constant independent of the charge generation process. Using the Langevin approximation the recombination constant can be found [3]

$$k_R = \frac{q(\mu_p + \mu_n)}{\varepsilon_0 \varepsilon_r} \tag{3}$$

where q is the elementary charge, μ_p and μ_n the mobilities of the positive and negative ions, ε_0 the permittivity of vacuum and ε_r the dielectric constant of the medium considered.

The dissociation constant will depend on the electric field according to Onsager theory [4]. Here the applied electric field will lower the potential barrier binding negative and positive ions into ion pairs.

$$k_D = k_D^0 F(E) = k_D^0 \frac{I_1(4b)}{2b} \tag{4}$$

$$b = \sqrt{\frac{q^3 E}{16\pi\varepsilon_0\varepsilon_r k^2 T^2}} \tag{5}$$

where I_1 is the modified Bessel function of first order, E the electric field strength, k Boltzmann's constant and T the absolute temperature. The field enhancement function $F(E)$ is further plotted in Figure 5 using a dielectric constant of 2.2 for oil. It should be noted that b is rather sensitive to the value of the temperature.

From equation (2) assuming thermodynamic equilibrium we get that

$$k_D^0 = k_R \frac{n_0^2}{c} \tag{6}$$

The concentration of the ions at thermodynamic equilibrium is further defined by the ohmic conductivity of the oil

$$p_0 = n_0 = \frac{\sigma}{q(\mu_n + \mu_p)} \tag{7}$$

If an electric field is applied over the medium, the ions in it will be subjected to electrostatic forces that cause them to drift. The drift speed of the ions will be

$$\vec{w}_{p,n} = \mu_{p,n}\vec{E} \tag{8}$$

The drift of the ions might create an inhomogeneous ion distribution that will cause a diffusion of the ions as well. The diffusive fluxes are further proportional to the gradient of the ions densities with a proportionality coefficient equal do the diffusion coefficients of the ions. The diffusion coefficients can be found with Einstein's relation:

$$D_{p,n} = \frac{kT}{q}\mu_{p,n} \tag{9}$$

Equation (2) can now be extended by taking into account the drift and diffusion of ions, and by using (6) we get

$$\begin{cases} \dfrac{\partial p}{\partial t} + \nabla\left(\mu_p \vec{E} p - D_p \nabla p\right) = k_R n_0^2 F(E) - k_R p n \\ \dfrac{\partial n}{\partial t} - \nabla\left(\mu_n \vec{E} n + D_n \nabla n\right) = k_R n_0^2 F(E) - k_R p n \end{cases} \tag{10}$$

From the drift and diffusion of the ions we can also define the ion current density:

$$J_p = q\left(\mu_p \vec{E} p - D_p \nabla p\right), \qquad J_n = q\left(\mu_n \vec{E} n + D_n \nabla n\right),$$
$$J_{ion} = J_p + J_n \tag{11}$$

There is also a displacement current density present due to the time varying electric displacement field. This current will only be present in the transient part of the current, since the electric displacement field no longer changes at steady-state.

$$\vec{J}_{displacement} = \frac{\partial \vec{D}}{\partial t} = \varepsilon_0 \varepsilon_r \frac{\partial \vec{E}}{\partial t} \quad (12)$$

Adding up the ionic and displacement current density we get the total current density

$$\vec{J}_{tot} = \vec{J}_{ion} + \vec{J}_{displacement} \quad (13)$$

To calculate the resulting current in an external circuit connected to the electrodes in the system, the total current density has to be integrated over the surface of the electrodes.

Finally, since the charge transport equations (11) and the displacement current are dependent on the electric field, we also need Poisson's equation to calculate the electric potential from the space charge density.

$$\nabla(\varepsilon_0 \varepsilon_r \nabla\phi) = -q(p - n), \qquad \vec{E} = -\nabla\phi \quad (14)$$

2.2 Ion Injection

Earlier studies of conduction in dielectric liquids have shown that besides the dissociation of ions in the bulk of the liquid there is also an injection of ions from the electrodes [5]. The mechanism behind this injection is not yet completely understood but the behavior of the injection has been modeled for some dielectric liquids [6]. Injection from electrodes with insulating coating has also been observed [7] and the theory behind it will be used to try to describe the possible existence of ion injection from the oil-pressboard interface. The description of ion injection now follows.

2.2.1 Electrical double layer

Let us assume that we have two parallel-plate electrodes submerged into oil, over which no external electric field is applied. At the interface between the oil and the conducting surfaces of the electrodes a redistribution of charges will occur and this will lead to the formation of an electrical double layer as illustrated in Figure 2.

The first layer is the surface layer which consists of ions of one polarity being adsorbed directly to the conducting surface through chemical interactions. Which polarity the ion will have in the surface layer is determined by the physicochemical properties of the liquid-electrode interface and is generally not known. The ions in this layer are however strongly bound to the electrode and will therefore not be able to move around. In Figure 2 the polarity of the surface layer has been assumed as negative.

The second layer consists of ions being attracted through the Coulomb force to the surface layer. This means that the layer mostly consists of ions having a polarity opposite of that of the surface layer, but there are also charges of the other polarity present to some extent. Since the second layer consists of free ions it is much more loosely bound to the conducting surface. The ions will therefore start moving under the influence of externally applied electric fields. This layer is called the diffuse layer.

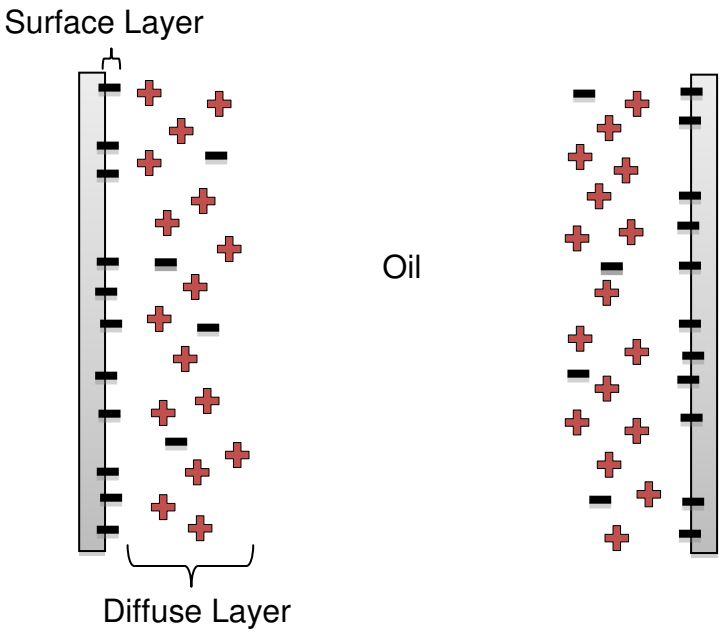

Figure 2. The formation of electrical double layer in the oil near the electrodes is illustrated.

2.2.2 Injection of Ions from the Electrical Double Layer

The ions compromising the diffuse layer will be at the bottom of a potential well due to the electrostatic attraction to their image charge at the electrode surface. Some of these ions will escape this potential well. If there then is an electric field applied over the electrodes, the escaped ions will start to drift in the direction of the electric field. This is illustrated in Figure 3 and Figure 4. In these figures it is once again assumed that the surface layer consists of negative ions. The ions which are in majority in the diffuse layer will give rise to the dominant injection. A weak injection will also be caused by the ions of the opposite polarity. Increasing the applied field will lower the potential barrier, and in this way more ions will escape the potential barrier.

The process of how ions are injected from a layer of charges close to metal contacts has been studied and modeled in earlier studies [8]. How ions are regenerated in such a layer is not completely known. It can however be described by a transfer reaction of ion pairs near the electrodes [9]. In the vicinity of the electrodes ion pairs are attached by the electrostatic image force. Through a charge transfer reaction between the electrode and the ion pair, the ion pair will be dissociated and reduction or oxidation of one of the resulting ions will occur. The other ion constituting the ion pair will become a part of the charge layer and can later be injected into the bulk of the oil. In a charge layer injecting positive charges, the following reaction would yield a regeneration of the charges.

$$A^+B^- \rightarrow A^+ + B + e^- \tag{15}$$

Here A^+ and B^- are assumed to be the same ions as in equation (1) which means that they can take part in recombination reactions with the ions in the bulk.

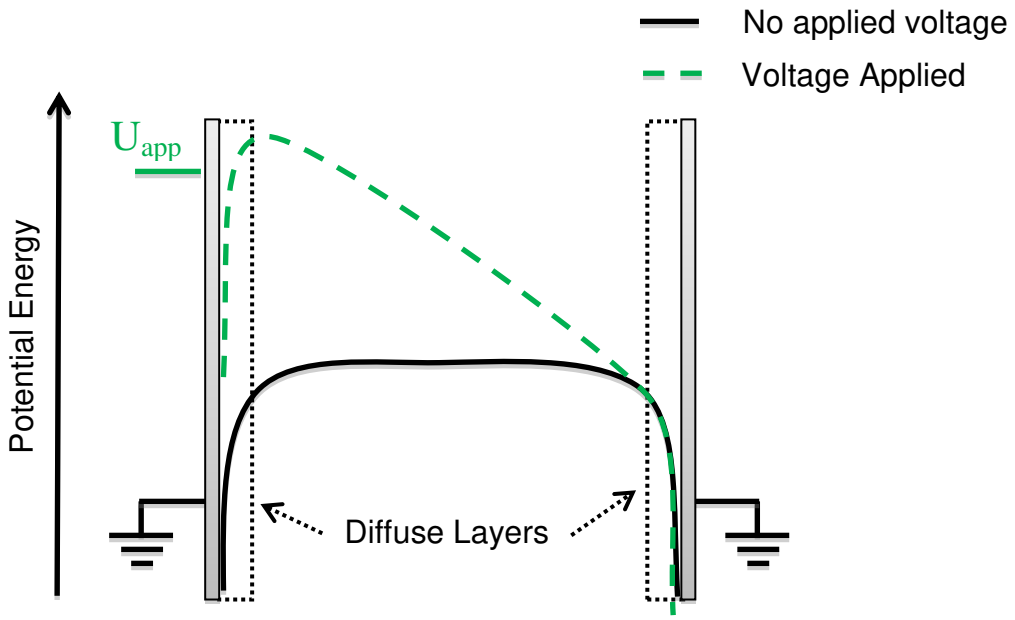

Figure 3. Electrical potential curves for oil gap when no voltage is applied (black line) as well as when voltage is applied (green dashed line)

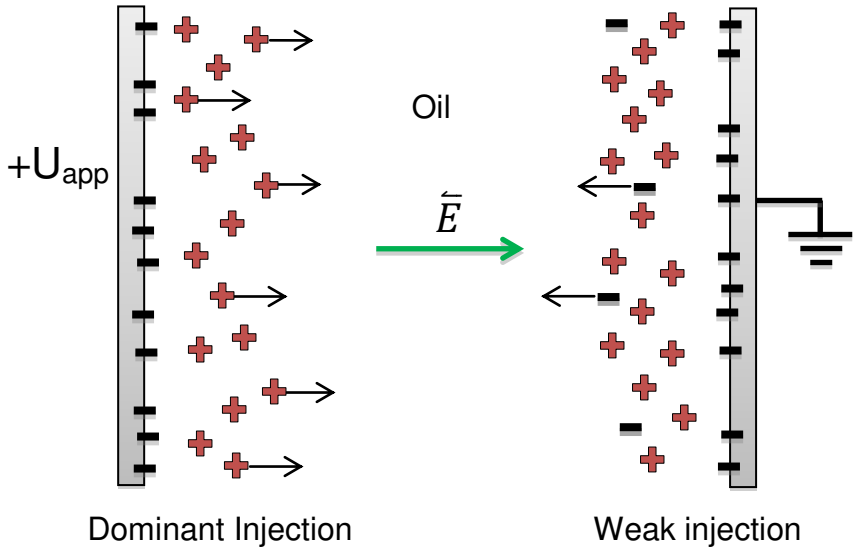

Figure 4. Electrical double layer injecting ions

2.2.3 Sign of Dominant Injection

Since the polarity of the surface layer in the double layer is generally unknown, it is not clear which polarity of the electrodes that gives the strongest injection. So this has to be determined somehow. One way of determining the sign of the dominant injection is to use a wire and a coaxial cylinder as suggested in [10]. Alternatively the electric field distribution can be measured in the oil-gap between two parallel plate-electrodes as a function of position. By observing at which electrode the electric field is the lowest, the electrode giving rise to the dominant injection can be determined. These approaches will be treated in more detail later on.

2.2.4 Apparent Injection from Electrodes

Injection of ions from the double layer at the oil-electrode interface will be referred to as apparent injection of ions from the electrodes. This is to clarify that it's actually not an injection from the electrodes but from the double layer. It will now be assumed that the charge concentration in the diffuse layer is in equilibrium, meaning that ions being sent off directly are replaced by ions being generated through equation (15). The following expressions can then be derived for the injected charge density due to the escape of ions from the double layer [9].

$$\begin{cases} p_{inj} = A_{pos} p_0 F_i(E) = A_{pos} p_0 \dfrac{1}{2bK_1(2b)} \\ n_{inj} = A_{neg} n_0 F_i(E) = A_{neg} n_0 \dfrac{1}{2bK_1(2b)} \end{cases} \tag{16}$$

Here K_1 is the modified Bessel function of the second kind and order one and A_{pos} and A_{neg} are constants defining the injection strength. A positive unipolar injection will be obtained by setting $A_{neg} = 0$ while a negative unipolar injection can be obtained by setting $A_{pos} = 0$. Allowing both injection strength parameters to differ from zero will give rise to a bipolar injection. Assuming a unipolar injection, the injection strengths have been found to be in the order of unity in most of dielectric liquids [9]. The expression for b defined in (5) should be evaluated at the electrode the charges are being injected from. The function $F_i(E)$ is plotted in Figure 5 using a dielectric constant of 2.2 for oil. Using equation (7) again, equation (16) can be rewritten as

$$\begin{cases} p_{inj} = \dfrac{A_{pos}\sigma}{q(\mu_p + \mu_n) \cdot 2bK_1(2b)} \\ n_{inj} = \dfrac{A_{neg}\sigma}{q(\mu_p + \mu_n) \cdot 2bK_1(2b)} \end{cases} \tag{17}$$

The injected current densities can now be determined from the injected charge density

$$\begin{cases} \vec{J}_p^{inj} = q\mu_p p_{inj} \vec{E}_{sur} \\ \vec{J}_n^{inj} = q\mu_n n_{inj} \vec{E}_{sur} \end{cases} \tag{18}$$

Here $\vec{E}_{sur}$ is the electric field at the surface of the injecting electrode.

2.2.5 Apparent Injection from Non-Metal Interfaces

In the oil at an interface between oil and pressboard, there will also be a formation of a double layer. This double layer will inject ions into the oil and through this process ions will also be injected into the pressboard. This injection will be referred to as apparent as well to distinguish it from ions that really are being transported through the interface. The injection can be modeled in the same way as before, but the liquid permittivity in the expression of the field enhancement has to be changed. This is due to the permittivity presented by the pressboard, which will alter the image force barrier. The effective permittivity is given by [7]

$$\varepsilon_{ap} = \varepsilon_{oil} \frac{\varepsilon_{pb} + \varepsilon_{oil}}{\varepsilon_{pb} - \varepsilon_{oil}} \tag{19}$$

This gives the following new expression for b

$$b_{pb} = \sqrt{\frac{q^3 E}{16\pi\varepsilon_0\varepsilon_{oil} \dfrac{\varepsilon_{pb} + \varepsilon_{oil}}{\varepsilon_{pb} - \varepsilon_{oil}} k^2 T^2}} \tag{20}$$

And from this we can deduce the expression for the injected charge density into the oil

$$\begin{cases} p_{inj}^{into\ oil} = B_{pos} p_0 F_i'(E) = \dfrac{B_{pos}\sigma}{q(\mu_p + \mu_n) \cdot 2b_{pb} K_1(2b_{pb})} \\ n_{inj}^{into\ oil} = B_{neg} n_0 F_i'(E) = \dfrac{B_{neg}\sigma}{q(\mu_p + \mu_n) \cdot 2b_{pb} K_1(2b_{pb})} \end{cases} \tag{21}$$

Here B_{pos} and B_{neg} are constants corresponding to the constants A_{pos} and A_{neg}. The resulting field enhancement is now drastically reduced for large electric field strengths as can be seen in Figure 5. There a dielectric constant of 2.2 and 4.3 has been used for the oil and pressboard respectively.

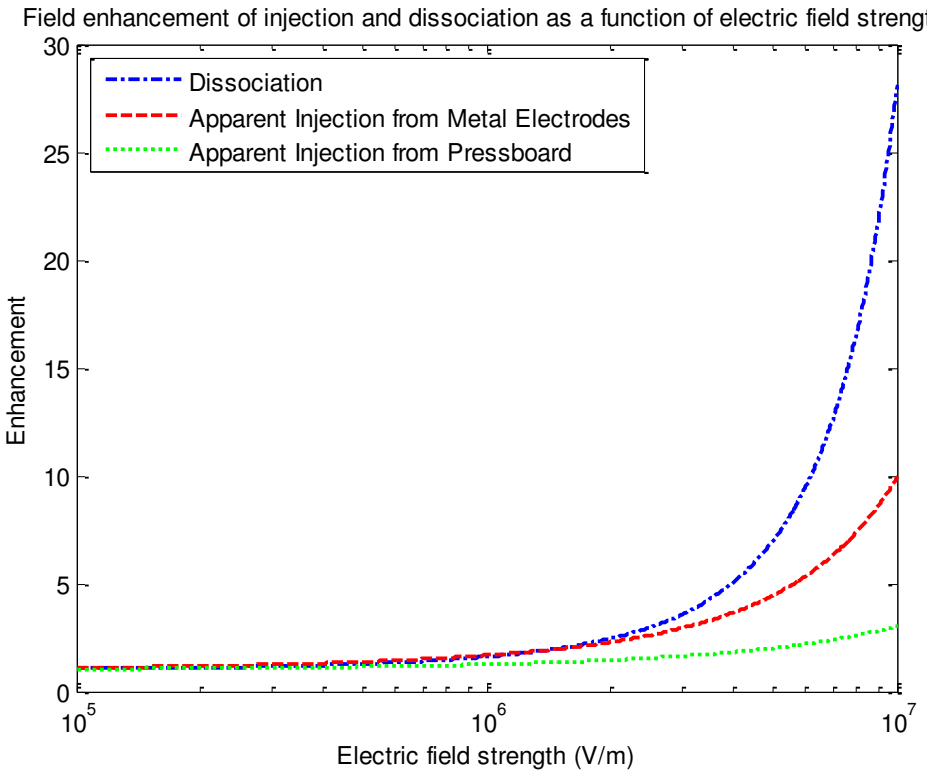

Figure 5. Field enhancement function F (dissociation), F_i (apparent injection from electrodes) and F_i' (apparent injection from oil-pressboard interfaces) plotted as a function of electric field strength at temperature 293K.

The injected positive ion flux from the pressboard into the oil will be

$$\phi_p^{inj\ into\ oil} = \mu^{oil} p_{inj}^{into\ oil} E_{sur}^{oil} \tag{22}$$

In contrast with the double layer at the oil-electrode interface, the other ions in the ion pairs will now be considered as well. They give rise to an injected charge flux of opposite polarity into the pressboard. This flux can be found by starting out from the equality of the flux injected into the oil and the flux injected into the pressboard.

$$\phi_p^{inj\ into\ oil} = \phi_n^{inj\ into\ pb}$$

$$\mu_p^{oil} p_{inj}^{into\ oil} E_{sur}^{oil} = \mu_n^{pb} n_{inj}^{into\ pb} E_{sur}^{pb}$$

$$\mu_p^{oil} p_{inj}^{into\ oil} \frac{D}{\varepsilon_0 \varepsilon_r^{oil}} = \mu_n^{pb} n_{inj}^{into\ pb} \frac{D}{\varepsilon_0 \varepsilon_r^{pb}}$$

By further requiring the D-field to be continuous over the boundary we get the following relation for the injected positive charge

$$n_{inj}^{into\ pb} = \frac{\varepsilon_r^{pb}\mu_p^{oil}}{\mu_n^{pb}\varepsilon_r^{oil}} p_{inj}^{into\ oil} \tag{23}$$

Similarly, in the case of negative injection, we get

$$p_{inj}^{into\ pb} = \frac{\varepsilon_r^{pb}\mu_n^{oil}}{\mu_p^{pb}\varepsilon_r^{oil}} n_{inj}^{into\ oil} \tag{24}$$

2.3 Delimitation of insulation system

When the ions in the oil/pressboard reach the electrode of opposite charge, there is a charge transfer reaction that involves the electrons in the external circuit. The nature of these reactions is not known and is therefore not modeled. Instead it's assumed that these reactions occur instantly when the ions reach the electrodes. This simplification is carried out by excluding the electrodes from the studied system. Thereby the current in the external circuit has to be calculated by integrating the total current density consisting of the ionic and displacement current density over the boundary to the electrodes. This delimitation is illustrated in Figure 6. The whole double layer will not be a part of the modeled system; instead the ions injected from the diffuse layer will be injected directly from the boundary. By doing so the ion concentration in the diffusive layer is considered to always be in equilibrium.

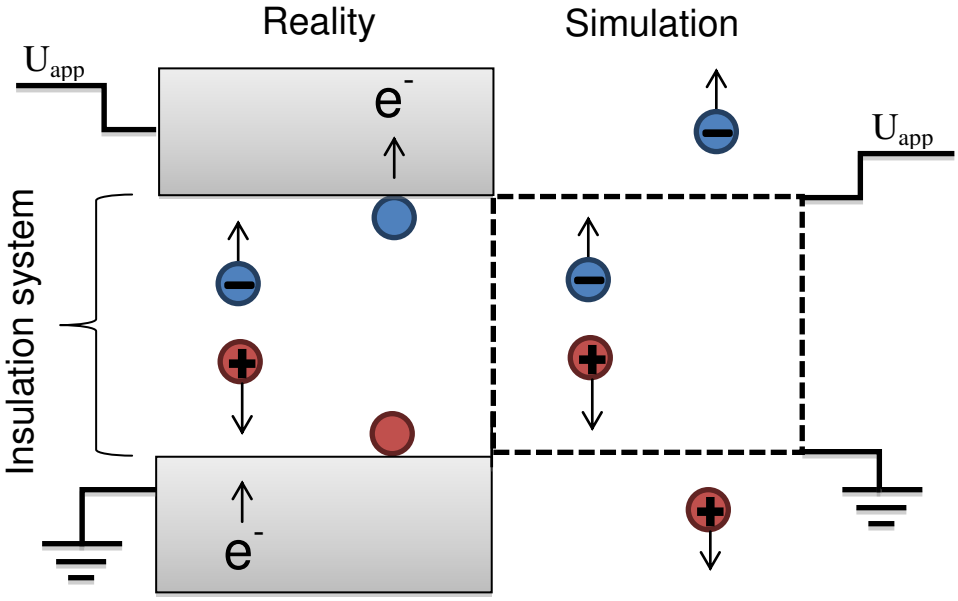

Figure 6. Illustration of delimitation

2.4 Boundary conditions

Solving equation (10) and (14) for a particular geometry requires conditions being supplied for the boundaries. For non-metal boundaries, we will assume no gradient in charge density perpendicular to the boundary and also that the D-field is parallel to the boundary at the boundary.

2.4.1 Oil-Metal Boundaries

Depending on the direction of the flux, the boundary condition at the oil-metal boundary will be different. If the flux of ions is directed towards the boundary, the charges will be transferred to the external circuit after having reached the contact. This can be achieved by requiring the total flux of ions to be continuous on the boundary. If the flux on the other hand is directed away from the contact, the injection of ions will be used as the

boundary condition. The injected flux of ions is given by $\mu_n n_{inj}\vec{E}_{sur}$ or alternatively $\mu_p p_{inj}\vec{E}_{sur}$.

2.4.2 Oil-Pressboard Internal Boundaries

The flux of the ions passing through the oil-pressboard boundary has to be continuous. On the oil side the flux is given by

$$\begin{cases} \phi_p^{oil} = p_{oil}\mu_p^{oil}E^{oil} = p_{oil}\mu_p^{oil}\dfrac{D}{\varepsilon_0\varepsilon_r^{oil}} \\ \phi_n^{oil} = n_{oil}\mu_n^{oil}E^{oil} = n_{oil}\mu_n^{oil}\dfrac{D}{\varepsilon_0\varepsilon_r^{oil}} \end{cases}$$

These fluxes have to be equal to the fluxes on the pressboard side

$$\begin{cases} \phi_p^{pb} = p_{pb}\mu_p^{pb}E^{pb} = p_{pb}\mu_p^{pb}\dfrac{D}{\varepsilon_0\varepsilon_r^{pb}} \\ \phi_n^{pb} = n_{pb}\mu_n^{pb}E^{pb} = n_{pb}\mu_n^{pb}\dfrac{D}{\varepsilon_0\varepsilon_r^{pb}} \end{cases}$$

By further demanding the D-field to be continuous over the boundary, we get the following relations

$$\begin{cases} p_{oil} = k_p p_{pb} = \dfrac{\mu_p^{pb}\varepsilon_r^{oil}}{\mu_p^{oil}\varepsilon_r^{pb}}p_{pb} \\ n_{oil} = k_n n_{pb} = \dfrac{\mu_n^{pb}\varepsilon_r^{oil}}{\mu_n^{oil}\varepsilon_r^{pb}}n_{pb} \end{cases} \tag{25}$$

So the complete injection condition for the oil-pressboard boundary consists of the actual injection of ions through the interface together with the apparent injection from the oil-pressboard interface. The existence of an apparent injection into the oil from the interface will include the associated apparent injection into the pressboard from the interface. These boundary conditions are summarized in Table 1 and also illustrated in Figure 7.

Table 1. Boundary conditions for Oil-Pressboard interface

	E-field directed from the oil into the pressboard		E-field directed from the pressboard into the oil	
	Positive Injection	Negative Injection	Positive Injection	Negative Injection
p_{oil}	given by internal flux	given by internal flux	$k_p p_{pb} + p_{inj}^{into\ oil}$	$k_p p_{pb}$
n_{oil}	$k_n n_{pb}$	$k_n n_{pb} + n_{inj}^{into\ oil}$	given by internal flux	given by internal flux
p_{pb}	$\frac{1}{k_p}p_{oil}$	$\frac{1}{k_p}p_{oil} + \frac{\varepsilon_r^{pb}\mu_n^{oil}}{\mu_p^{pb}\varepsilon_r^{oil}}n_{inj}^{into\ oil}$	given by internal flux	given by internal flux
n_{pb}	given by internal flux	given by internal flux	$\frac{1}{k_n}n_{oil} + \frac{\varepsilon_r^{pb}\mu_p^{oil}}{\mu_n^{pb}\varepsilon_r^{oil}}p_{inj}^{into\ oil}$	$\frac{1}{k_n}n_{oil}$

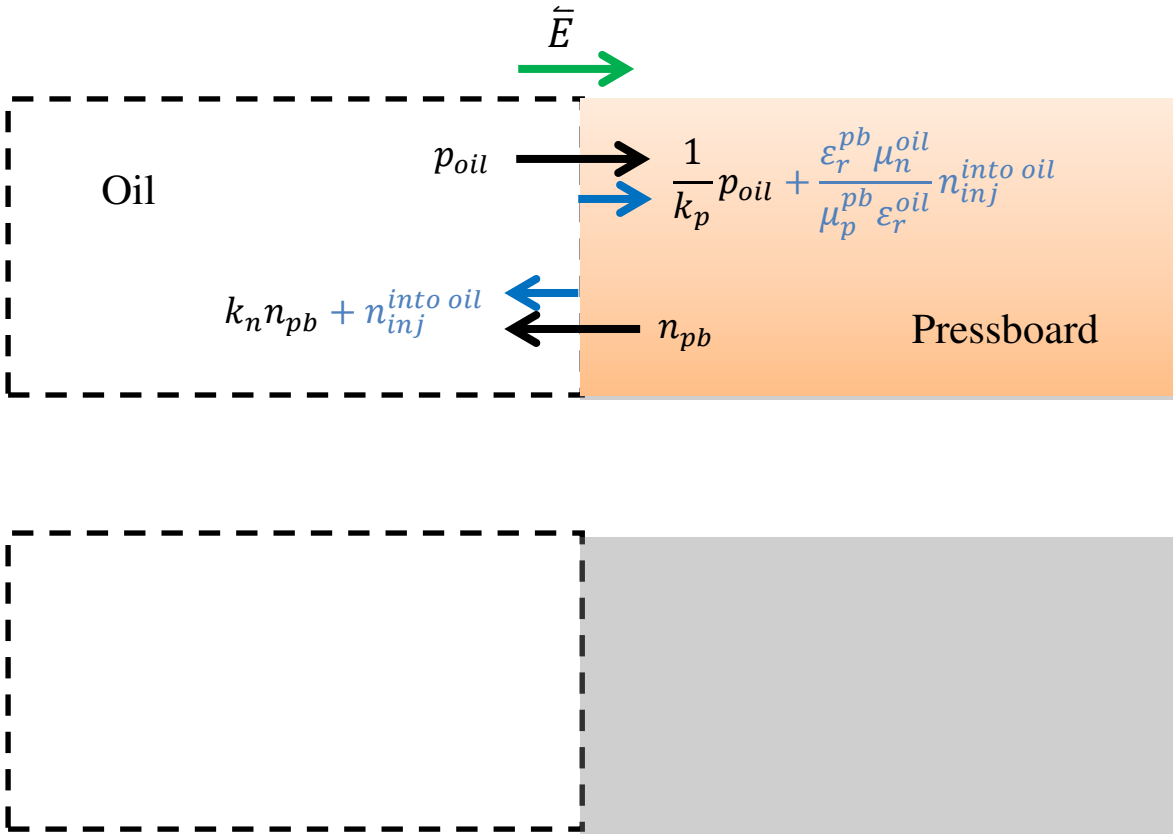

Figure 7. Visualization of the boundary condition of the oil pressboard boundary depending on the direction of the E-field. The blue terms are only contributed if there is a negative injection into the oil from the interface and the red terms if there is a positive injection into the oil from the interface.

2.5 Characteristics of the Oil and the Pressboard

The oils used in transformers are normally a complex mixture of paraffinic, naphthenic and aromatic hydrocarbons. The dielectric constant for these oils is about 2. The oil-impregnated pressboard, which consists of cellulose fibers and pores filled with oil, is much more resistant to electric breakdown. Due to the complex structure of the pressboard, the ion mobility therein will be much lower than in oil. This also leads to a much higher resistivity of the pressboard. The oil and the pressboard are both modeled by the equations presented earlier except that no field enhancement of the dissociation is used in the pressboard. The parameters used for the simulations are presented in Table 2.

Table 2. Material parameters used for simulations

Material	Mobility ($\mu = \mu_p = \mu_n$)	Resistivity ρ	Dielectric constant ε_r	Initial ion concentration
Oil	$10^{-9}\mathrm{m}^2/\mathrm{Vs}$	$3 \cdot 10^{13}\ \Omega m$	2.2	$1 \cdot 10^{14}\ m^{-3}$
Pressboard	$10^{-15}\mathrm{m}^2/\mathrm{Vs}$	$3 \cdot 10^{15}\ \Omega m$	4.3	$1 \cdot 10^{18}\ m^{-3}$

3 EXPERIMENTAL DATA USED FOR VALIDATION

For the validation of the ion injection model, experimental data from 5 different test geometries were used. The first test geometry was basically an oil gap exposed to a uniform electric field by the application of a voltage over two parallel plate electrodes. This geometry, called Case 1, is used to better study the transport and generation as well as the injection of ions in the oil and how this affects the electric field therein. A further development of this is Case 2, which consist of an oil gap with a pressboard barrier. The idea with studying this geometry is to better understand how charges are building up in the pressboard and thereby affecting the electric field distribution in the system. The third test geometry, Case 3, aims at further studying these phenomena under irregular electric fields. The last two geometries were two coaxial versions of Case 1 used to study the sign of the injection. All the test geometries are illustrated in Figure 8.

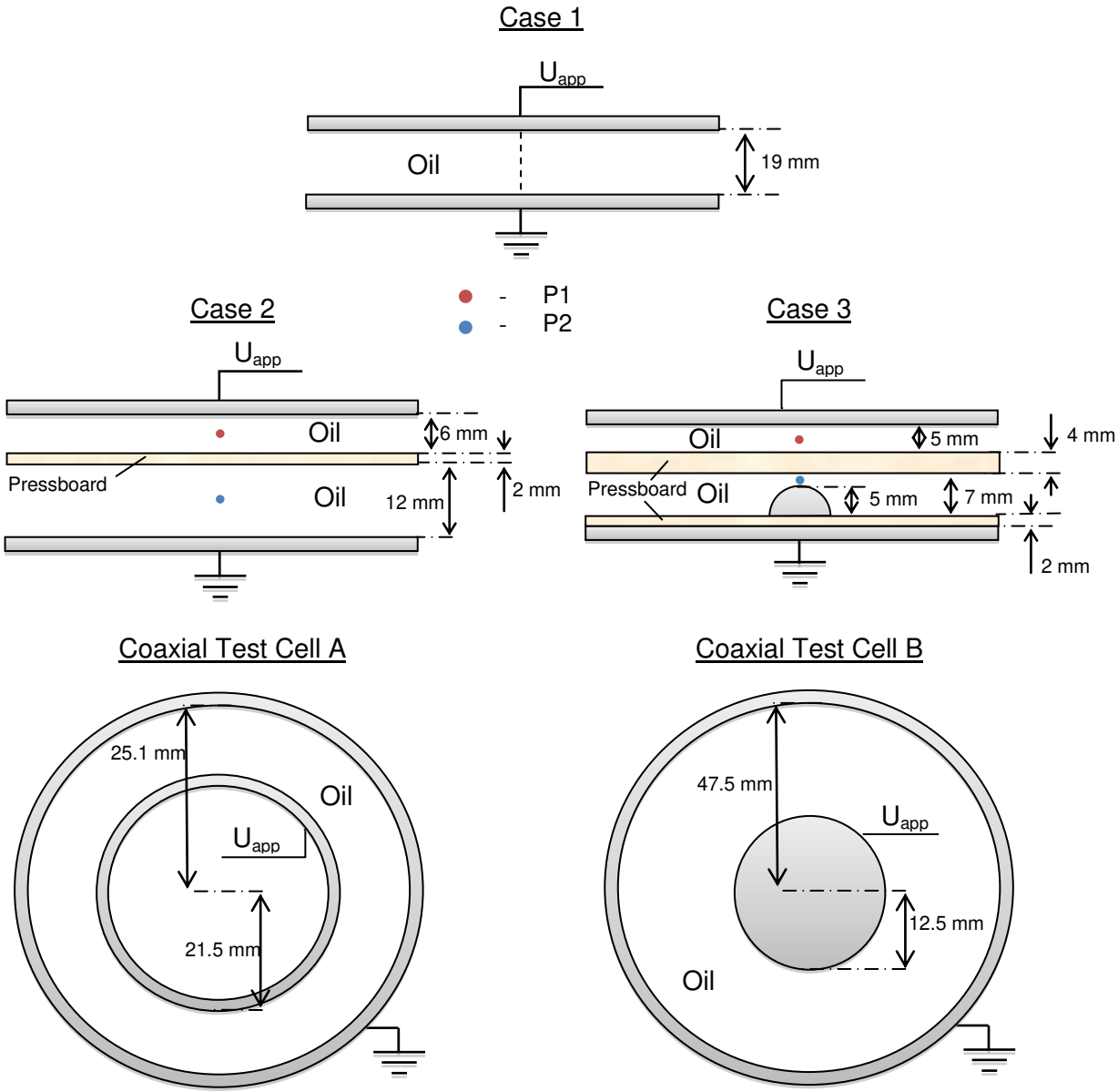

Figure 8. Illustrations of the different test geometries used

In parallel to this master thesis, an investigation of measurement techniques for finding the polarity of ion injection in transformer oil was made [12]. In the investigation the two different coaxial test cells were used. The height of Coaxial Test Cell A was 8.6 cm and the height of Coaxial Test Cell B 13 cm. The idea behind these geometries was to have

an inhomogeneous electric field having different values of the electric field at the two electrodes. That way the effect of the injection will be different depending on which electrode it's coming from. The electric field distributions for the two coaxial test cells are illustrated in Figure 9. These electric fields are calculated under the assumption that there are no charges in the oil. We can see that the electric field at the two electrodes is differing much more for coaxial test cell B.

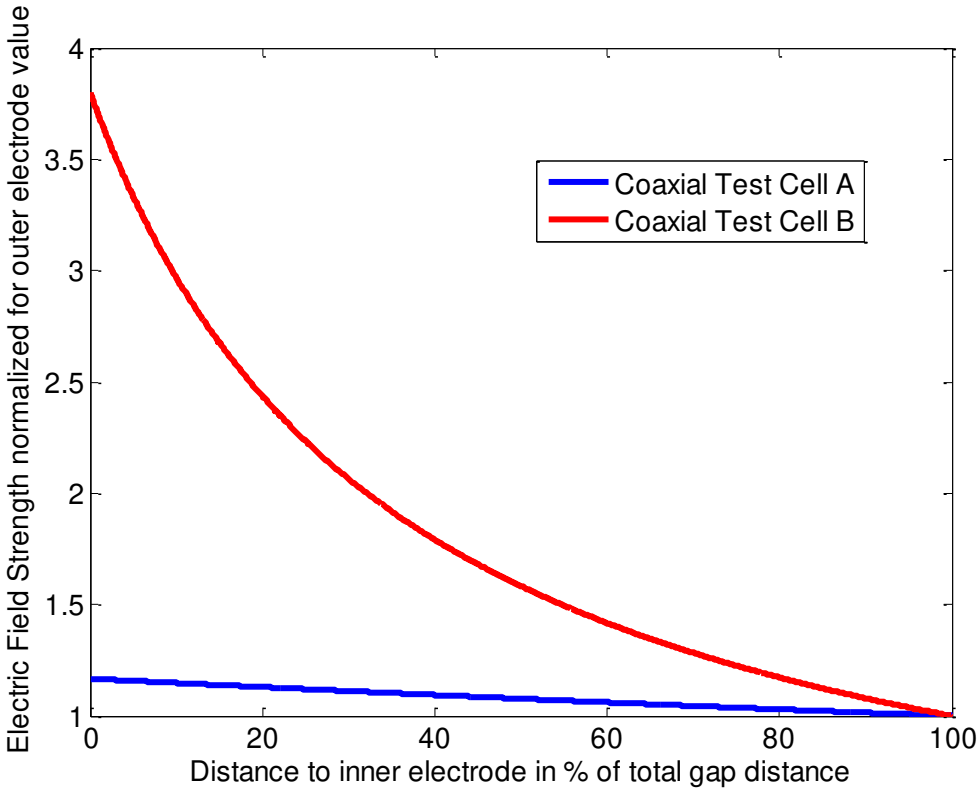

Figure 9. Electric fields in the coaxial test cells normalized for the outer electrode values, assuming no space charges.

3.1 Acquisition of Experimental Data

Data of the electric field for case 1, 2 and 3 were acquired through Kerr Measurements, working as follows. When an electric field is applied over a medium, a birefringence is induced in the medium. The optical axis is given by the direction of the electric field. This is called the electro-optic Kerr effect. Sending a beam of polarized light through the medium will cause a phase shift between the polarization component perpendicular and parallel to the optical axes. By measuring the phase shift the electric field can be determined. [1]

The physical quantity measured for the coaxial versions for Case 1 was the current through the external circuit when a voltage was applied over the electrodes. More information about the experimental set-up can be found in [12].

3.2 Case 1: Blank Oil Gap in Uniform Field

Measurements done in [1] made it possible to validate the ion drift diffusion model for a simple oil gap. The gap distance between the electrodes used was 19 mm. Shown in Figure 10 is the Kerr measurements compared with calculated curves from the ion drift model (not including injection) for different voltages. The positive electrode is at position 0 while the negative is at 1. The measurements were made along the dashed line shown

in Figure 8. In this study a transformer oil was used with a conductivity of $0.5 \cdot 10^{-12}\ (\Omega m)^{-1}$. Although the curves match very well for low voltages, there is a considerable deviation for the higher voltages. This deviation could be explained by an injection of charges from one of the electrodes.

We notice that there is an increase of the electric field strength relative to the calculated one when approaching the negative electrode. Having a concentration of positive ions being overall higher than that from calculations would explain this deviation. Assuming this overall increase in positive ion concentration is due to a unipolar injection, we can further conclude that the injection must come from the positive electrode. This since a negative electrode not possibly could inject positive charges.

Apart from concluding a positive sign of the injection in this case, an estimation of the injection magnitude can also be made. Proceeding from the data in Figure 10 for 20kV, it can be seen that the total increase in the electric field strength from the positive electrode to the negative is about 70kV/m. This increase is not influenced by the generation and recombination of charges in the oil since this gives rise to a symmetric electric field distribution in the gap. The estimated increase in electric field strength can further be used to calculate a mean derivative of the D-field with respect to the position in the oil gap:

$$\frac{dD}{dx} = \frac{dE}{dx}\varepsilon_r^{oil}\varepsilon_0 \approx \frac{\Delta E}{\Delta x}\varepsilon_r^{oil}\varepsilon_0 = \frac{70\,\frac{\mathrm{kV}}{\mathrm{m}}}{0.019\mathrm{m}} \cdot 2.2 \cdot 8.854 \cdot 10^{-12}\,\frac{F}{m} \approx 7.5 \cdot 10^{-5}\,\frac{\mathrm{F \cdot kV}}{\mathrm{m^3}}$$

By using Poisson's equation (14), the corresponding increased ion density can be calculated.

$$p_{inj} = \frac{\frac{dD}{dx}}{q} = \frac{7.5 \cdot 10^{-5}\,\frac{\mathrm{F \cdot kV}}{\mathrm{m^3}}}{1.6022 \cdot 10^{-19}C} \approx 4.7 \cdot 10^{14} m^{-3}$$

By assuming that this concentration is injected from the positive electrode, the injection magnitude can be estimated

$$A_{pos} = \frac{p_{inj}}{n_0} = \frac{4.7 \cdot 10^{14} m^{-3}}{1.6 \cdot 10^{15} m^{-3}} \approx 0.3$$

Taking the field enhancement for the injection into account will instead yield

$$A_{pos} = \frac{p_{inj}}{n_0 F_i(E)} = \frac{4.7 \cdot 10^{14} m^{-3}}{1.6 \cdot 10^{15} m^{-3} \cdot 1.7} \approx 0.2$$

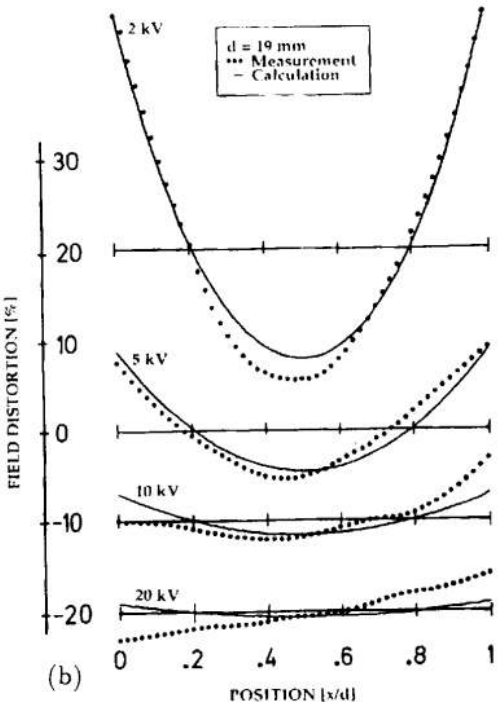

Figure 10. The relative field distortion for four different voltages and the corresponding calculated curves from ion drift model without ion injection. Conductivity $0.5 \cdot 10^{-12}$ $(\Omega m)^{-1}$ [1].

3.3 Case 2: Oil Gap with Pressboard Barriers in Uniform Field

Measurements of the electric field for Case 2 with an applied voltage of 20kV have been studied earlier at ABB Corporate Research in Västerås. Oil with the resistivity of around $3 \cdot 10^{-13}$ was used. The electric field was then measured as a function of time in the middle of the two oil gaps (in point P1 and P2 shown in Figure 8). The measurements that were obtained are presented in Figure 11 together with a simulation of the ion drift diffusion model without injection. The curves are somewhat similar for the 12000 first seconds but then there is a turn in the experimental curve for point P2, which makes the curves deviate more as time goes by.

Initially we see that the measured electric fields in the two oil gaps are equal. This is before the generation and transportation of ions in the system has given a spatial distortion of the electric field. After that, two things can be noticed for the transient of the measured electric field strengths. Firstly the electric field in the smaller gap is larger than that for the larger gap throughout time and secondly the electric fields in the two oil gaps have an overall decreasing trend. Both these observations can be explained by how charges are building up in the pressboard.

The buildup is mainly due to the difference in mobility, which causes the charges to move much slower in the pressboard than in the oil. The charges are able to pass through the oil gaps in a few seconds, while the pressboard takes ~20 days for the charges to pass through. This means that the buildup of charges will continuously increase until the first charges have started to pass through the pressboard. As long as this buildup is being increased, the electric field distribution will continue to be transferred to the pressboard. This explains the overall decrease of the electric field in the two oil gaps.

The larger oil gap further contains more volume of oil and therefore generates more charges through dissociation. This means that the larger oil gap will transfer more of its

electric field distribution to the pressboard compared to the smaller gap. So the larger oil gap will therefore have lower electric field strengths than the smaller oil gap.

In addition to the generation of charges in the oil, there could also be an injection of charges in the system which contributes to the buildup of charges in the pressboard. The effect of this contribution will later on be studied in simulations.

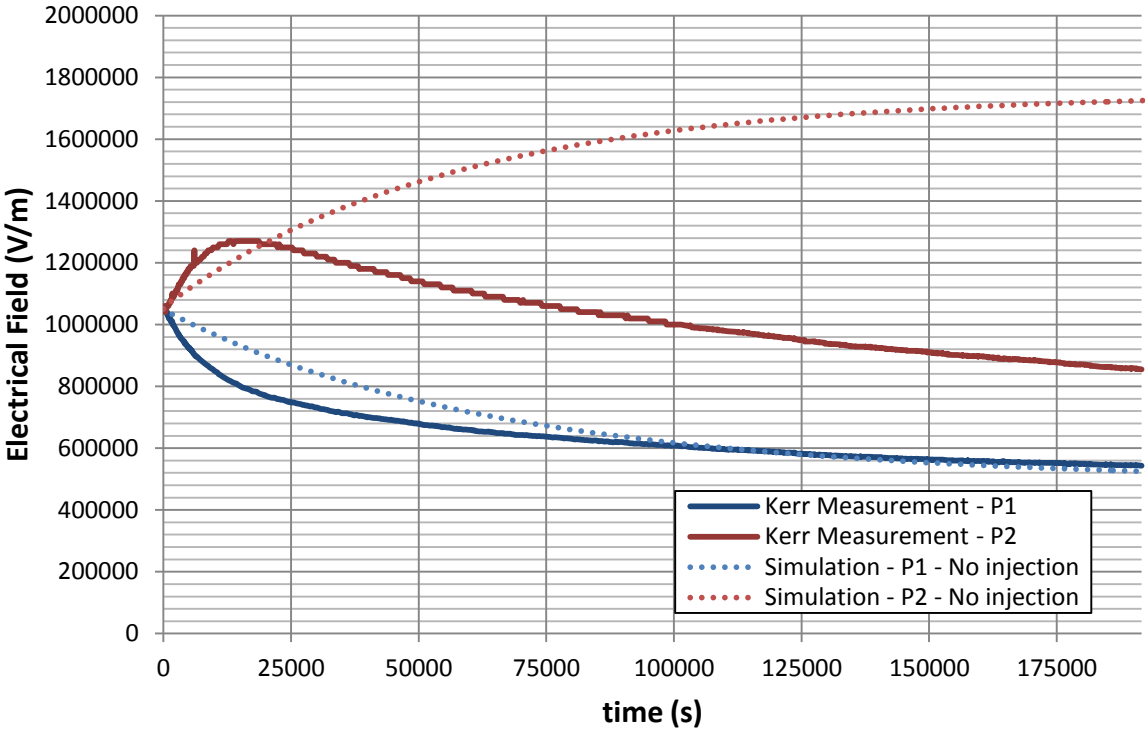

Figure 11. Kerr measurements for Case 2 compared with simulation from the ion drift diffusion model when 20kV is applied over the electrodes.

3.4 Case 3: Oil Gap with Pressboard Barriers in Divergent Field

The electric field strength in Case 3 has been studied for two points P1 and P2 in the same way as in Case 2. Point P1 and P2, shown in Figure 8, are situated in the lower oil gap 0.5 mm from the cylindrical protrusion and in the upper oil gap 3 mm from the upper electrode. The measurements were performed for both polarities of an applied voltage of 2kV. The resistivity of the oil used was around $3 \cdot 10^{-13}$, just like Case 2. The results of these measurements have been presented in [11] and can also be seen in Figure 12 and Figure 13 together with simulations of the ion drift diffusion model without injection.

Here we see that there is a strong dependence of the polarity of the applied voltage that the ion drift diffusion model does not capture. As can be seen in Figure 12, when the potential -2kV is applied to the upper electrode, the transient of the electric field behaves somewhat similar to the curves in case B. The curves do not start from the same position this time but this is due to the inhomogeneous electric field caused by the geometry. When the potential on the upper electrode is changed to 2kV there is a significant change in behavior, as can be seen in Figure 13. After about 1500 s it's no longer the smaller gap that has the largest electric field strength. A possible reason for the fast decrease in the electric field in P1 that will be further studied is that there could be a strong injection of charges into the smaller oil gap.

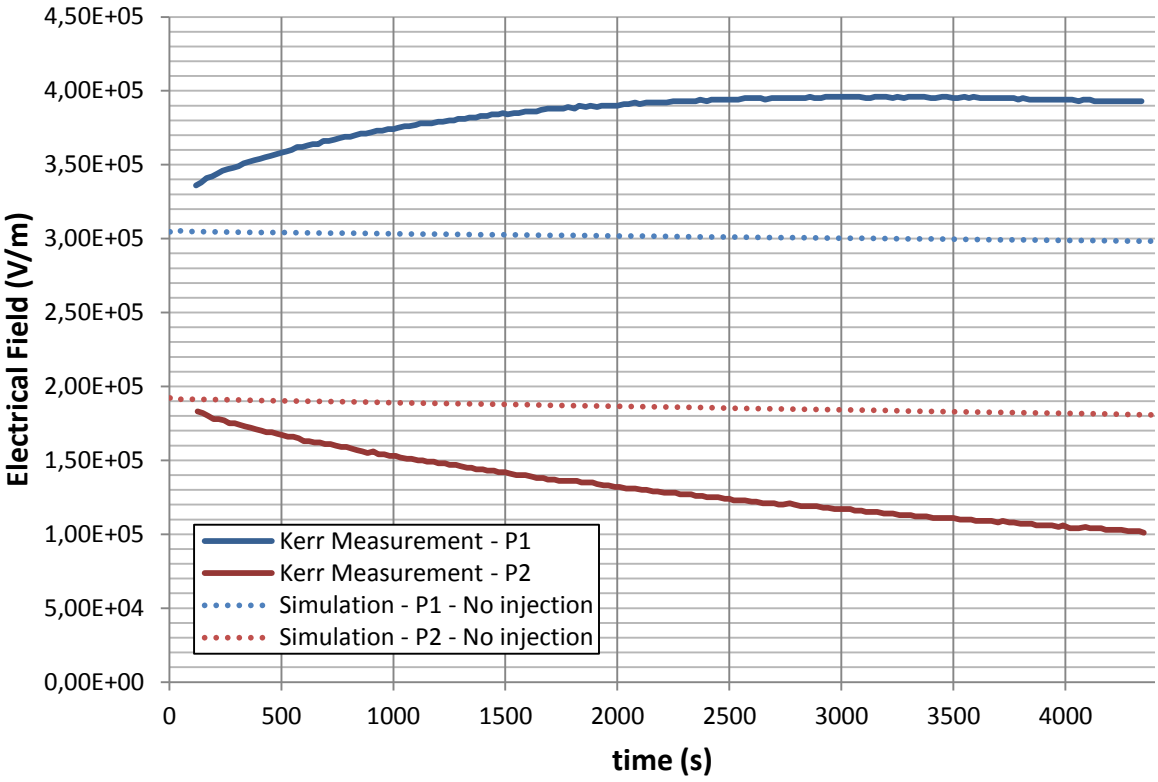

Figure 12. Kerr Measurements for Case 3 when the potential -2kV is applied to the upper electrode

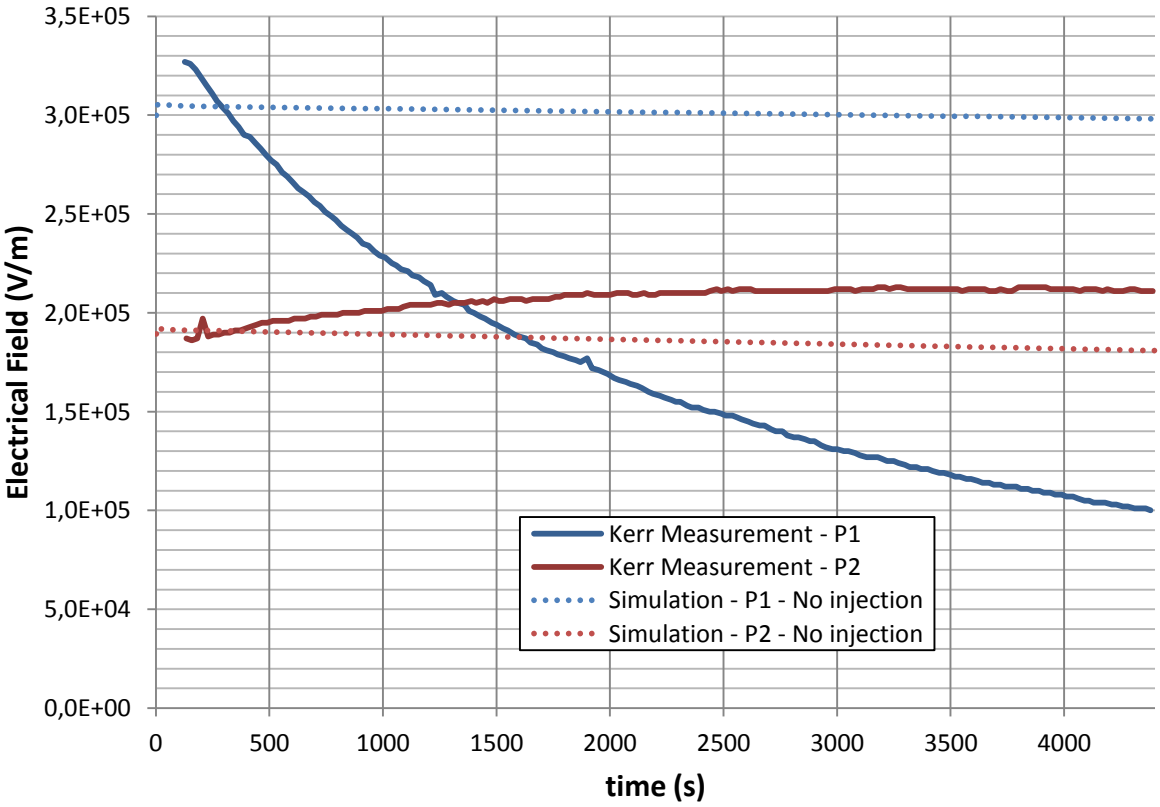

Figure 13. Kerr Measurements for Case D when the potential +2kV is applied to the upper electrode

3.5 Coaxial Test Cell A and B

Two different current measuring approaches were used to study the sign of the dominant injection from electrodes into transformer oil, both having advantages and drawbacks which will be discussed later. In both approaches, the current after application of voltages of different polarities was measured and compared. In the first approach, called Single Polarity Method, the test cell was grounded before application of the voltage. The grounding times needed to assure that the system was in a restored state was about 3 days. The results of the Single Polarity Method measurements for both coaxial test cells are presented in Figure 14 and Figure 15 [12].

The second approach is called the Reversed Polarity Method. Before the voltage is applied, the opposite polarity has been applied until a steady state has been reached. The result can be seen in Figure 16 and Figure 17 [12].

To get a better idea of the magnitude of the currents, current densities can be calculated for the saturation current at the inner and outer electrodes. For the curves in Figure 14 and Figure 16 the current densities are in the order of $4 \cdot 10^{-10} \frac{A}{m^2}$ at the inner and outer electrode. For the curves in Figure 15 and Figure 17, the current densities for the saturated current is roughly $6 \cdot 10^{-9} \frac{A}{m^2}$ at the outer electrode and $2 \cdot 10^{-8} \frac{A}{m^2}$ at the inner electrode.

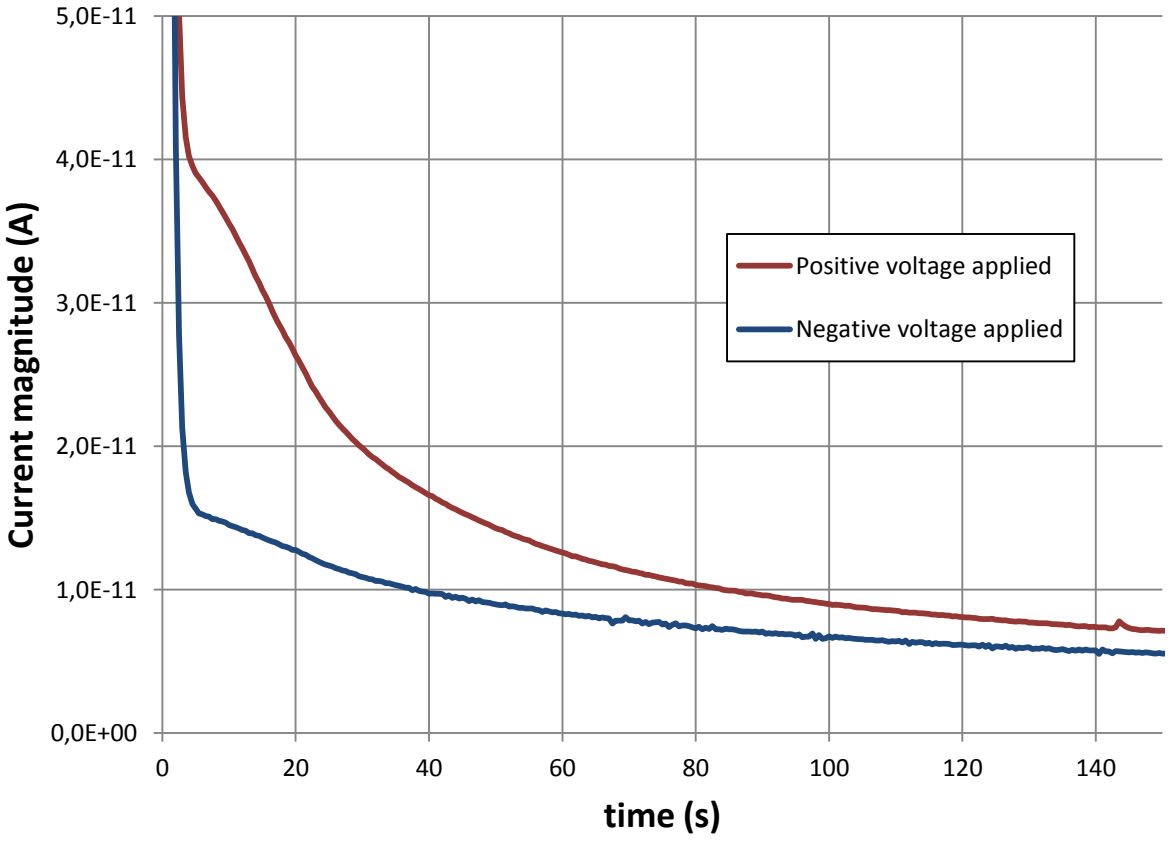

Figure 14. Coaxial Test Cell A – Single Polarity Method 400V: Measured current for different polarities of the applied voltage

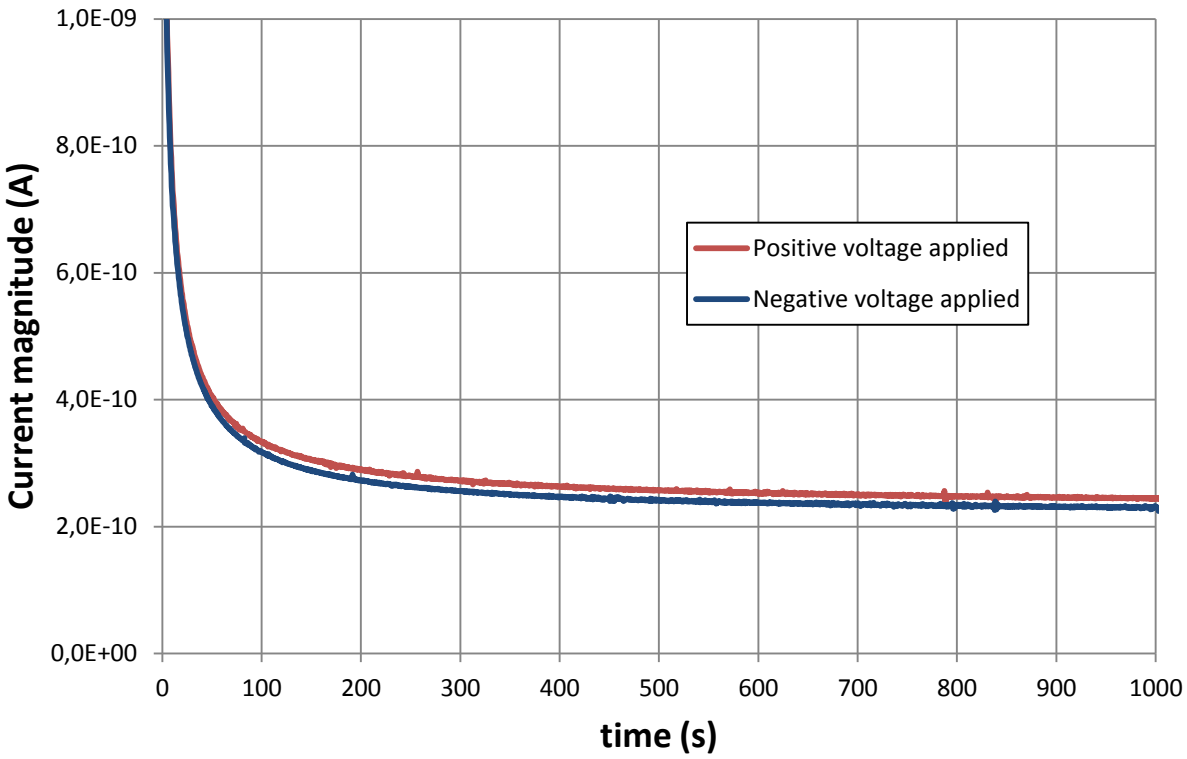

Figure 15. Coaxial Test Cell B – Single Polarity Method 1000V: Measured current for different polarities of the applied voltage

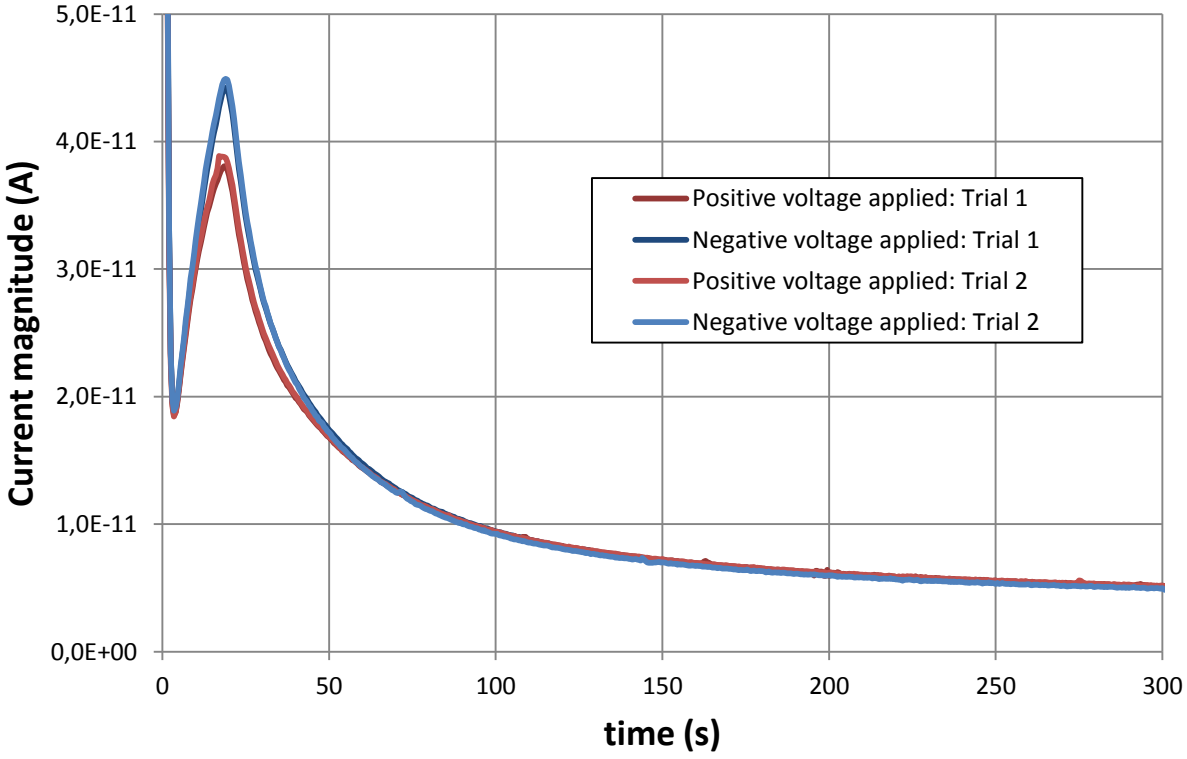

Figure 16. Coaxial Test Cell A – Reversed Polarity Method 400V: Measured current for different polarities of the applied voltage

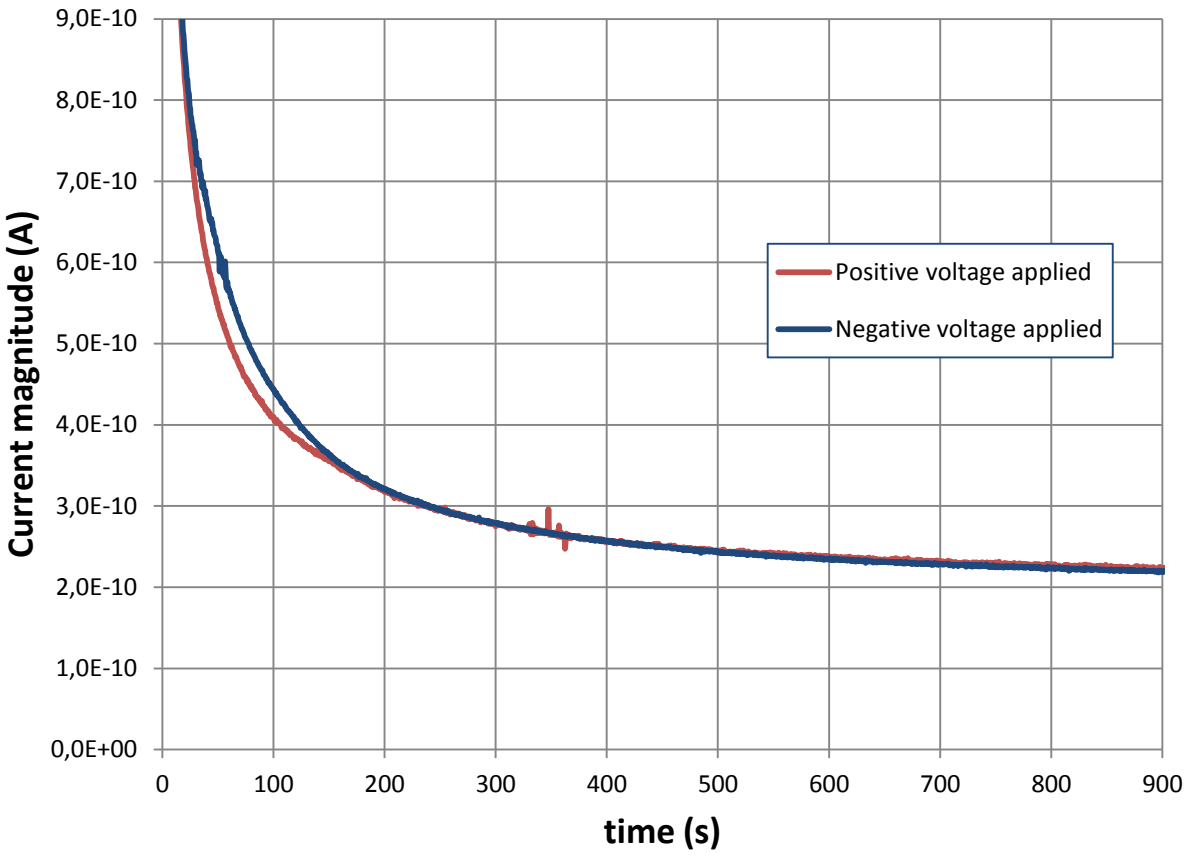

Figure 17. Coaxial Test Cell B – Reversed Polarity Method 1000V: Measured current for different polarities of the applied voltage

4 IMPLEMENTATION OF MODEL IN COMSOL MULTIPHYSICS

For solving the equation for the transport and generation of charges (10) together with Poisson equation (14) the FEM computational tool COMSOL Multiphysics ® version 4.2a was used. The reason behind this choice is that COMSOL Multiphysics® easily allows for coupling equations and well handles the nonlinearities that arise when solving these coupled equations together with non-linear boundary conditions. The geometry of the problems studied could easily be changed, which is favorable when studying different kinds of test cells. For equation (10) the module “Transport of diluted species” was used and for equation (14) the “Electrostatics” module.

4.1 Geometries

To minimize the computational effort when simulating for the different test geometries, all test geometries except Case 3 was simplified to 1D. Case 1 and 2 were solved along a line perpendicular to the electrode surface. For the coaxial test cells, the 1D axisymmetric space dimension was chosen to simulate the system for a line going radially from the inner to the outer electrode. Finally for Case 3, the 2D space dimension had to be chosen in COMSOL Multiphysics ® which resulted in considerably longer simulation times.

4.2 Generating Mesh

Generating the mesh for the geometries is a compromise. The mesh has to be fine enough to resolve the thin boundary layers. At the same time the mesh has to be kept coerce enough for the simulation to finish in a reasonable time. The optimal way to distribute the mesh elements is to put them densely close to boundaries to resolve the thin boundary layers and more sparsely in the bulk of the oil and the pressboard. The approach for choosing an appropriate mesh was to start by a coerce mesh and refine it until there no longer was any significant numerical error removed from the solution.

4.3 Time Stepping

When simulating the ion drift diffusion model the time stepping has to be fine enough to correctly capture the time evolution. Just like the meshing, the approach for choosing an appropriate time stepping was to start with a rough one and then decrease it until no longer any significant change was observed in the solution. It’s further important to notice that the longer the simulations are run the more important it is with a fine time step since the error is accumulated over time.

4.4 Stabilization of Solution

Due to the very high electric fields used for the studied insulation system, the transport part of equation (10) will be strongly dominated by convection. The lack of a physical diffusion in this problem will give rise to non-physical oscillations in the solution. These oscillations can be removed by adding an artificial diffusion to the problem. This extra diffusion will also alter the final solution and it is therefore important to set it as small as possible. In the oil an isotropic artificial diffusion of 0.5 was used while the diffusion in the pressboard was set 10 times smaller.

5 RESULTS OF SIMULATIONS

This section will start off with a basic study of how the charges in oil-pressboard insulation systems behave when subjected to electric fields. When this understanding has been established, the experimental results of Case 1, 2 and 3 will be compared with simulations of the ion drift diffusion model with the addition of the ion injection. This work will be focused on the study of unipolar injection, but the possibility of a bipolar injection will later be brought up in the discussion. For the test geometries containing both oil and pressboard, the effect of the apparent injection from the electrodes and the oil-pressboard interfaces are initially studied separately to see if that was enough to describe the experimental data. Thereafter the two injections are used together. Finally simulations for the coaxial test cells will be compared with the current measurements to allow for a better understanding of these results.

The approach for finding injection parameters giving a good fit to the experimental curves was done through trial and error. At first some parameters were chosen randomly, and based on the result of the simulations of them, new parameters were chosen. This approach was repeated until a sufficiently good match was attained.

5.1 Basic study of charge behavior

To better understand the behavior of the insulation systems consisting of oil and pressboard subjected to electric fields, two important processes affecting it will first be studied. The first process is the sweep-out of ions. The convection of ions due to the applied field is so high that the regeneration of ions isn't high enough to compensate for the ions drifting away. This will eventually deplete the ions in the bulk of the oil. This process is studied for Case 1 when the potential 20kV is applied to the upper electrode. How the ion densities are changing after the application of the voltage is shown in Figure 18. The difference between positive and negative ion densities times the electron charge defines the space charge density, which is shown in Figure 19. When the space charge density is no longer equal to zero, the electric field distribution will be distorted from its evenly distributed initial state. How the electric field is being distorted throughout time is shown in Figure 20. In all these figure, the y-position 0 corresponds to the lower electrode which is grounded and the y-position 0.019 corresponds to the upper electrode which has a potential of 20kV applied to it.

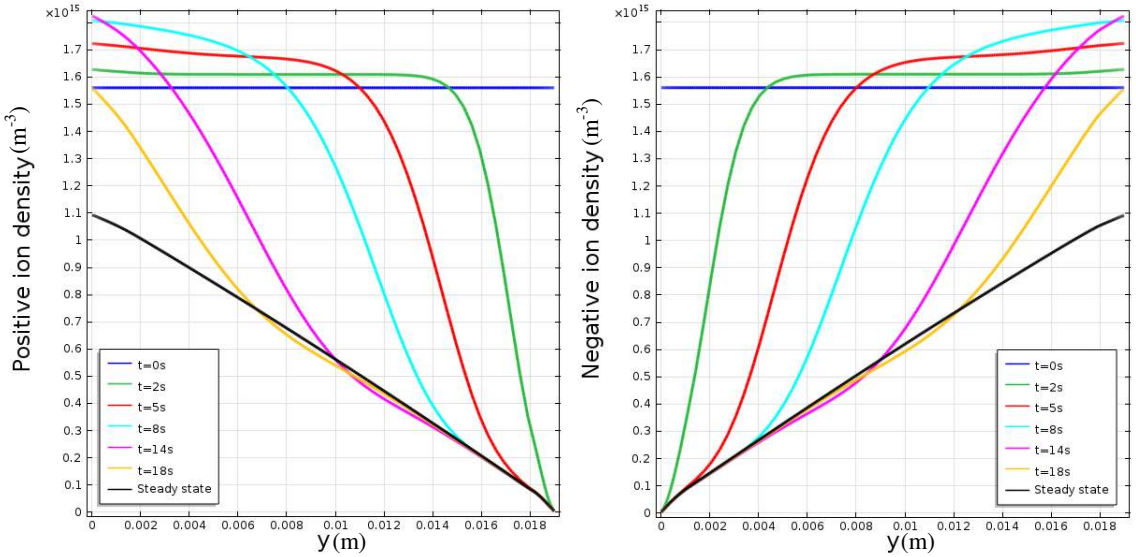

Figure 18. Time evolution of positive (left plot) and negative (right plot) ion densities for Case A when 20kV is applied.

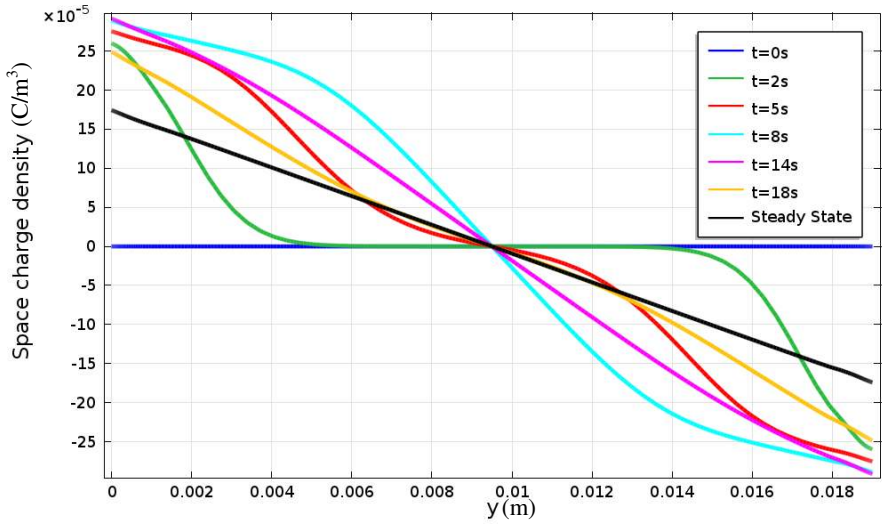

Figure 19. Time evolution of space charge density for Case A when 20kV is applied.

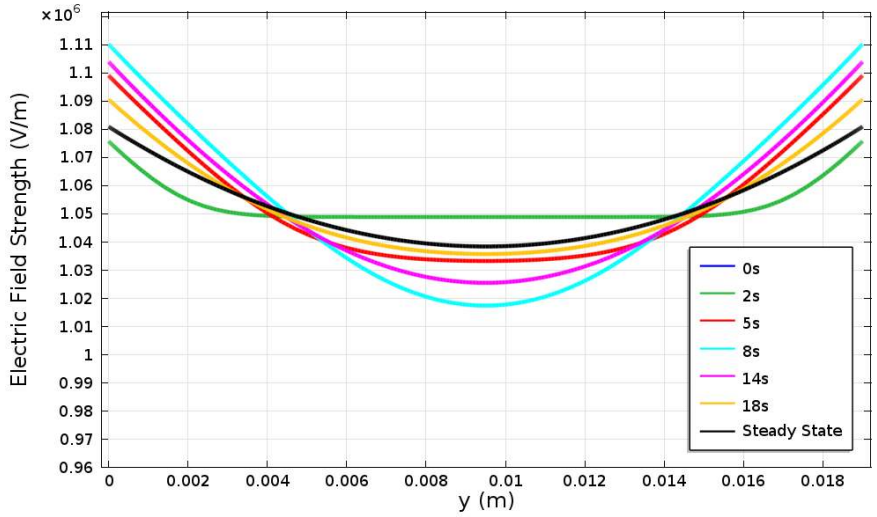

Figure 20. Time evolution of electric field distribution for Case A when 20kV is applied.

If pressboard is used in the system, there will also be process present consisting of the build-up of charges in the pressboard next to the pressboard-oil interface. This build-up is due to charges traveling much slower in the pressboard. Charges being transported from the oil to the pressboard will therefore slow down considerably when reaching the pressboard and build up a large charge peak which shifts the electric field distribution to the pressboard. This process is simulated with the ion drift diffusion model without injection for Case 2 with a potential of 20kV applied to the upper electrode. The resulting space charge density zoomed in on the pressboard is shown in Figure 21. It can be seen that the space charge build-up to the left in the plot is much larger than that to the right. The reason for this is that the oil gap providing this interface with charges is much larger, and hence generates more charges. The electric field associated with these space charge distributions are shown in Figure 22.

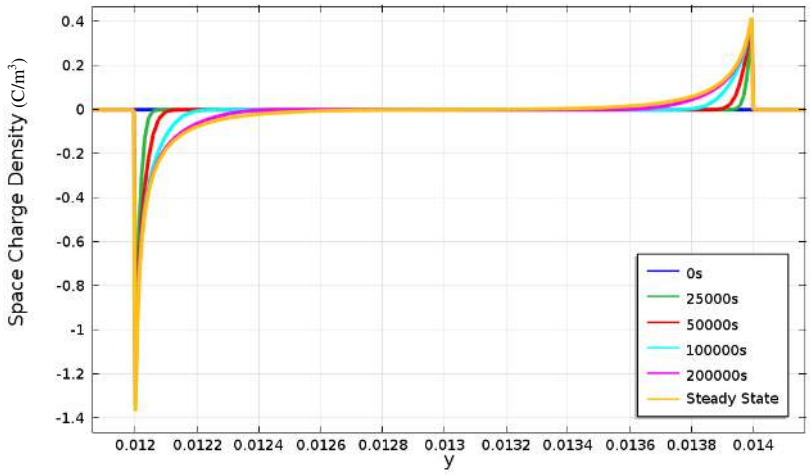

Figure 21. Time evolution of space charge density for Case 2 when a potential of 20kV is applied to the upper electrode.

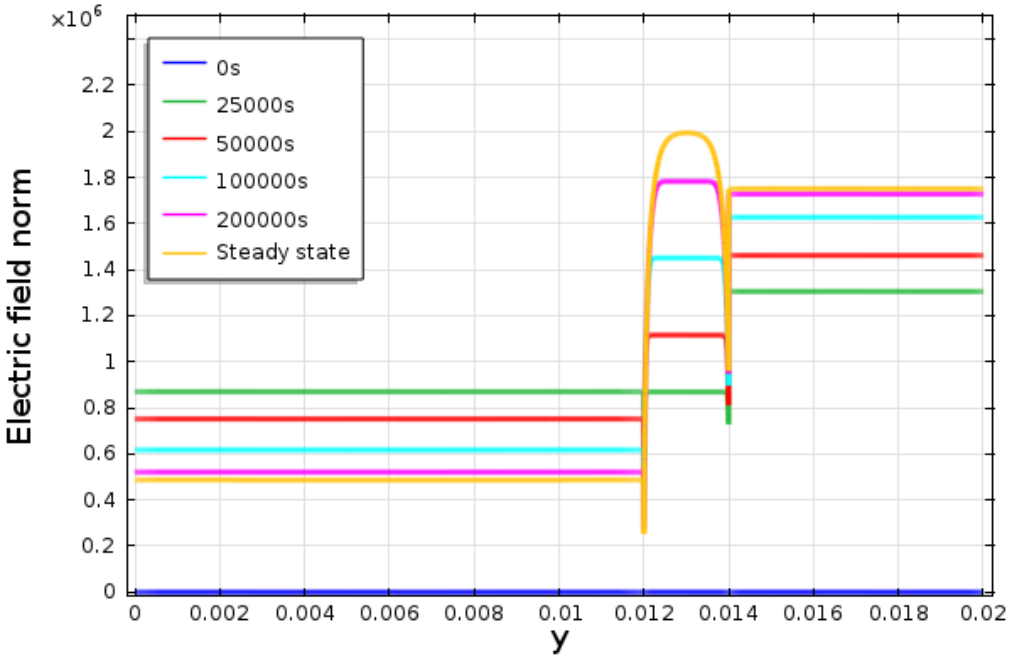

Figure 22. Time evolution of electric field distribution for Case 2 when a potential of 20kV is applied to the upper electrode.

5.2 Case 1: Blank Oil Gap in Uniform Field

As discussed before, the data earlier attained in [1] being presented in Figure 10, shows that the measurement of the electric field deviates from the simulation of the ion drift diffusion model without injection. The next step it to better catch this deviation by using the ion injection model. Only when a positive injection is used, it is possible to get a better match to the experimental data. In Figure 23 and Figure 24 the effect of three different injection levels are studied for 2kV and 20kV applied voltage. Comparing these plots with Figure 10 tells us that injection strength of around 0.3 gives the best match with the experimental data. This is in agreement with what was estimated in Section 3.2. Although the match isn't perfect, the injection model qualitatively explains the deviation from the ion drift diffusion model.

In Figure 10 it could be seen that the deviation from the ion drift diffusion model was much larger at 20kV than at 2kV. This can be explained by the field enhancement of the injection. Taking a look at Figure 5 we can see that the injection is enhanced by around 70% when 20kV is applied (corresponding to $\sim 10^6\ kV/m$). When 2kV is applied (corresponding to $\sim 10^5\ kV/m$), the field enhancement of the injection is negligible. In

Figure 25 and Figure 26 the corresponding figures without field enhancement of the injection is shown. The simulations for 2kV are about the same, but for 20kV the effect of the injection is decreased. It can be seen that it is not possible to match both the measurements for 2kV and 20kV for the same injection level when no field enhancement is used.

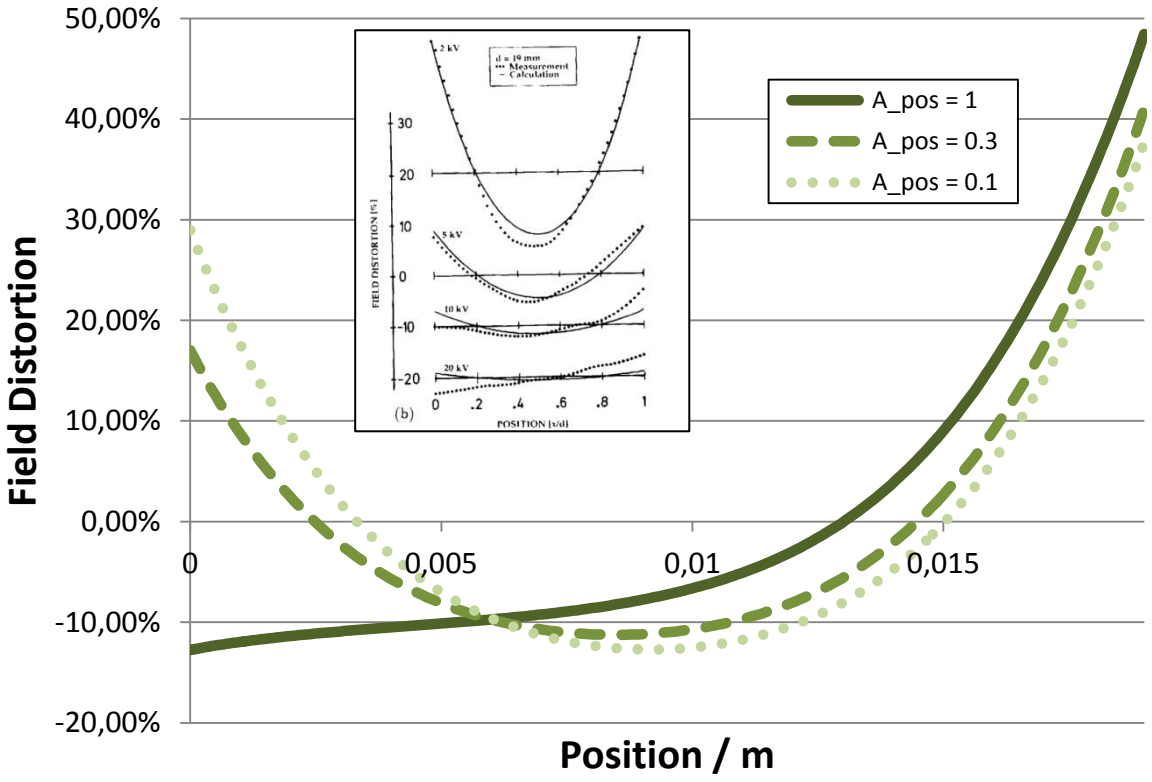

Figure 23. Case 1 with 2kV applied: Steady state electric field for different values of A_{pos} having a positive field enhanced injection from the electrodes. The resistivity of the oil is $2 \cdot 10^{12}\ \Omega m$.

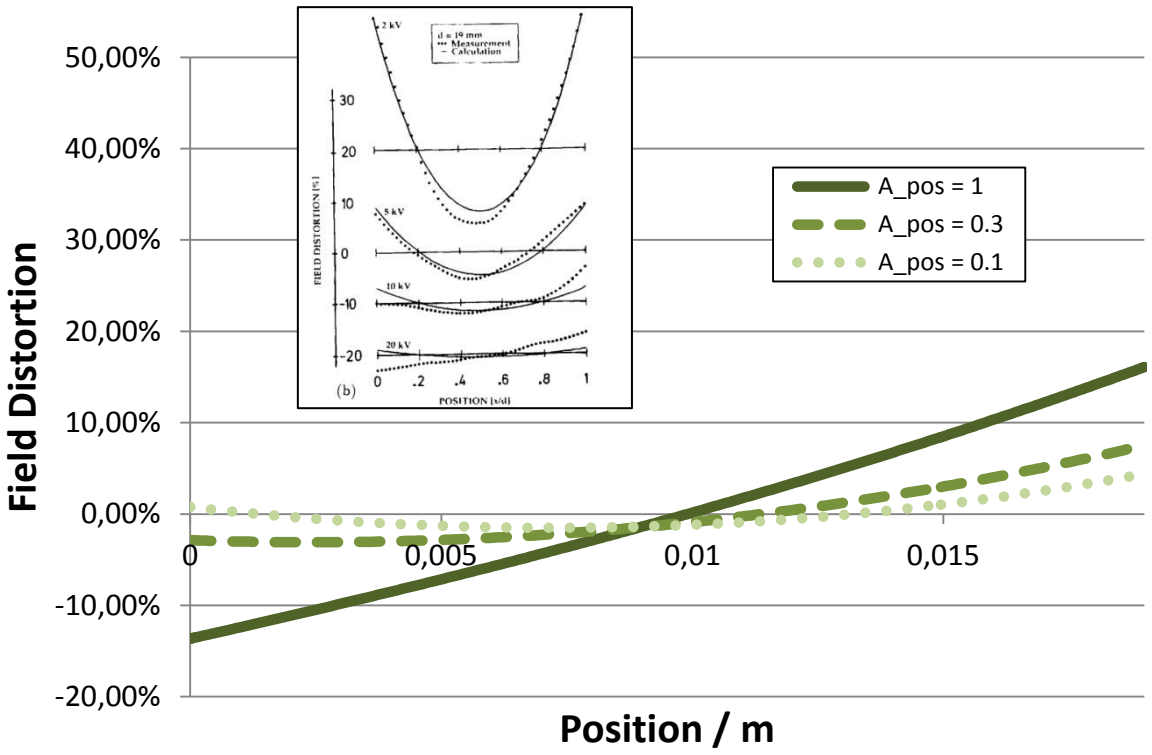

Figure 24. Case 1 with 20kV applied: Steady state electric field for different values of A_{pos} having a positive field enhanced injection from the electrodes. The resistivity of the oil is $2 \cdot 10^{12}\ \Omega m$

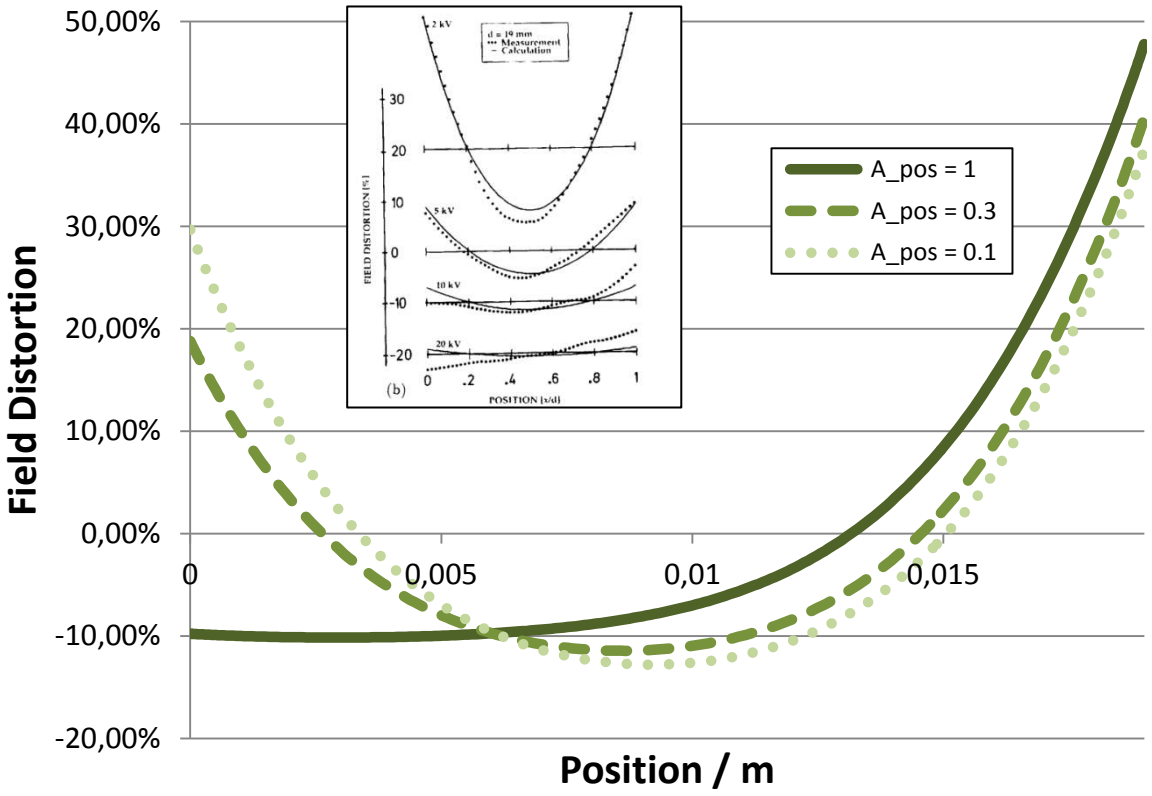

Figure 25. Case 1 with 2kV applied: Steady state electric field for different values of A_{pos} having a positive field independent injection from the electrodes. The resistivity of the oil is $2 \cdot 10^{12}\ \Omega m$

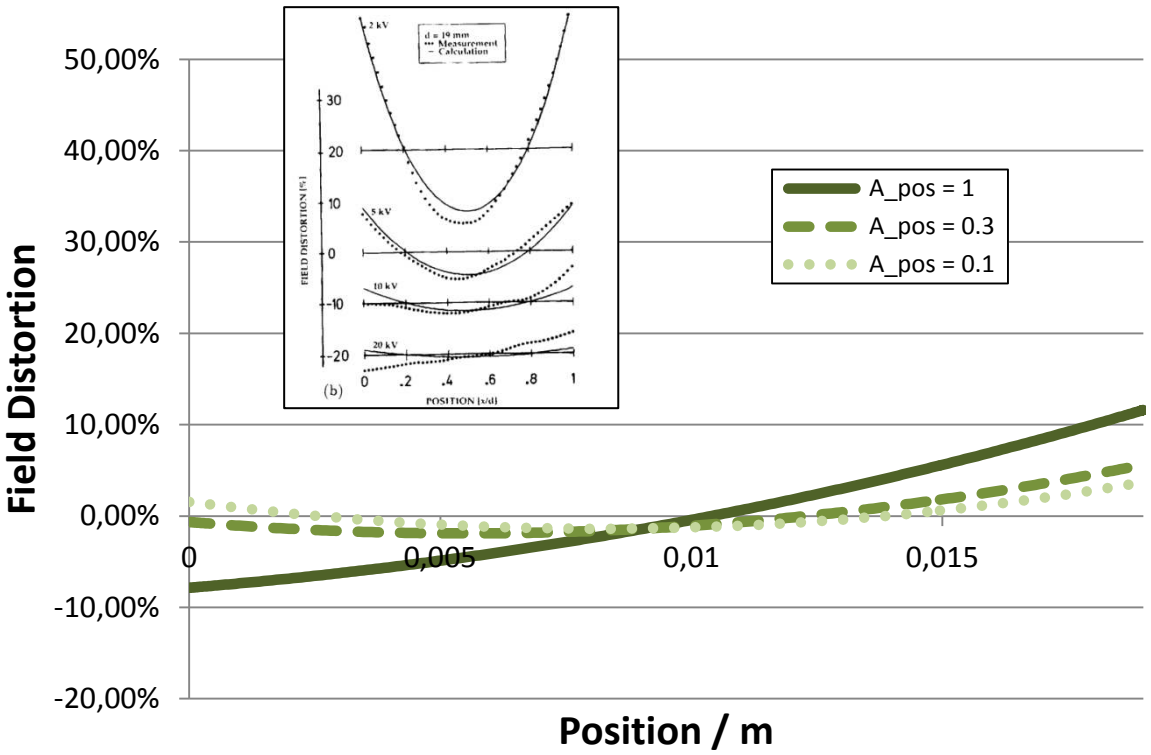

Figure 26. Case 1 with 20kV applied: Steady state electric field for different values of A_{pos} having a positive field independent injection from the electrodes. The resistivity of the oil is $2 \cdot 10^{12}\ \Omega m$

5.3 Case 2: Oil Gap with Pressboard Barriers in Uniform Field

As could be seen in Figure 11, the ion drift diffusion model without injection did not correctly describe the evolution of the electric field throughout time. The first extension that can be done to the simulation model is to add an injection from the electrodes. Both positive and negative injection was implemented and the result is presented in Figure 27 and Figure 28. The result of the injection is that the E-field in the gap where the charges are being injected is decreased. The important note here is that the same curvature as the experimental curve cannot be attained for any chosen value of the parameter of injection.

The next step was to investigate the effect of using only an injection from the oil-pressboard interface. The result is shown in Figure 29 and Figure 30. Just as for the injection from the electrodes, the E-field in the oil gap getting charges injected will decrease in a similar manner as before. This means that the curvature of the simulated electric field transient still is deviating from the experimental one.

Now both injections from the electrodes and the pressboard can be used together to try to get a better match of the experimental data. Since there are two possible sign of injection from the electrodes as well from the pressboard, this gives us 4 different combinations of implementation possibilities. In the case when one negative injection and one positive injection was used, meaning that all the injection occurred in one of the gaps, the result given was of the same nature as when only using injection from either the oil-pressboard interface or the electrodes. Neither of these cases brought anything further to the matching of the experimental curves.

If on the other hand, the same sign was used for the oil-pressboard and electrode injection, then a good fit to the experimental curves could be attained. This way there will

be injection in both oil gaps. The results for positive and negative injection are shown in Figure 31.

To further get an idea of how sensitive the solution is to changes in the resistivity, new simulations were performed for other oil resistivities. The result can be seen in Figure 32. It is interesting to see it that the simulated curves maintain the general curvature of interest. One important think to have in mind when studying this plot is that changing the resistivity will indirectly change the injection strength as well since the injection is defined as proportional to the initial ion concentration.

Finally the sensitivity for the injection magnitude parameters was investigated. The result of this is shown in Figure 33 and Figure 34. Also here the general curvature is kept for the values used.

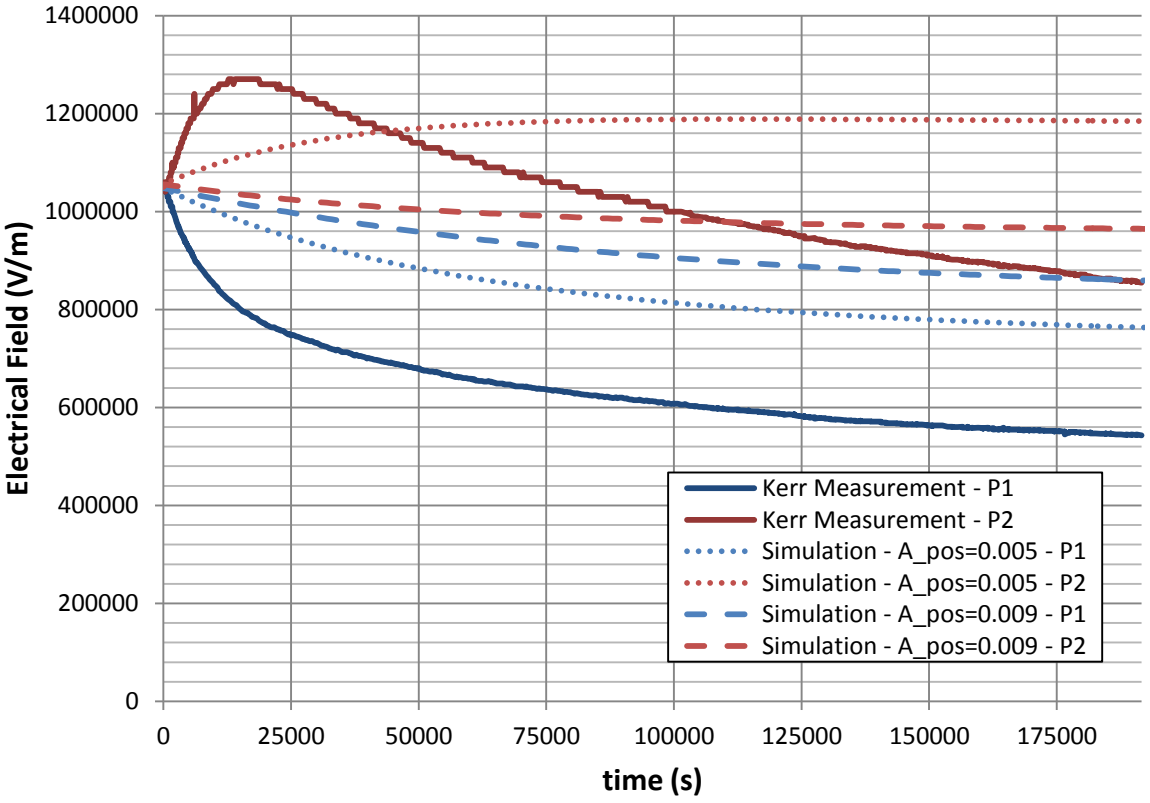

Figure 27. Case 2 +20kV: Simulation of ion drift diffusion model with positive injection from the electrodes

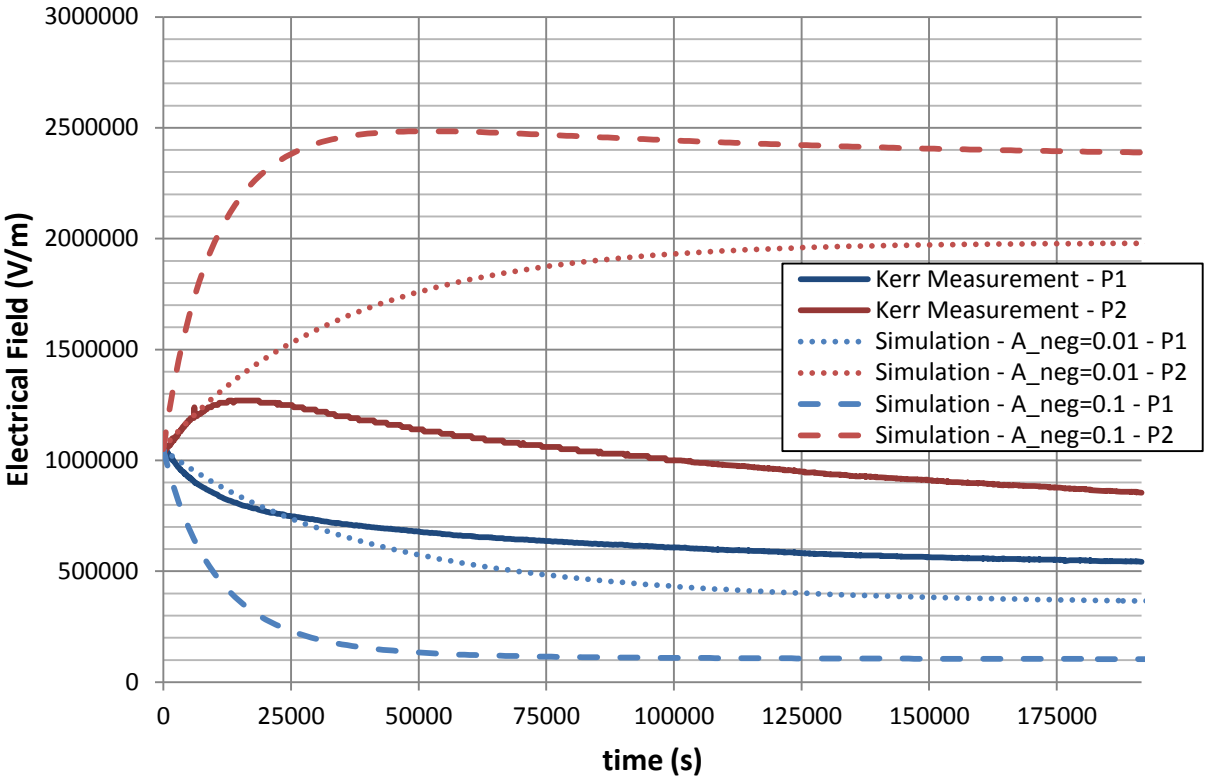

Figure 28. Case 2 +20kV: Simulation of ion drift diffusion model with negative injection from the electrodes

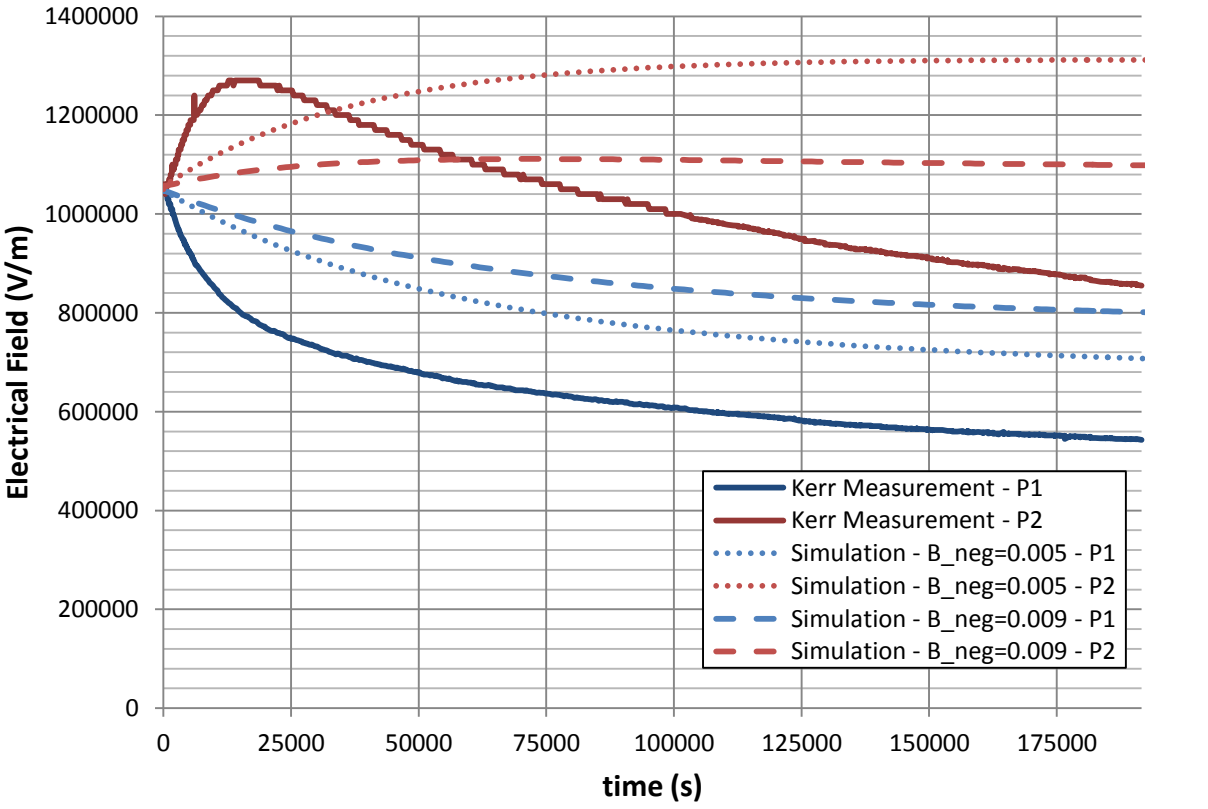

Figure 29. Case 2 +20kV: Simulation of ion drift diffusion model with negative injection from the oil-pressboard interface

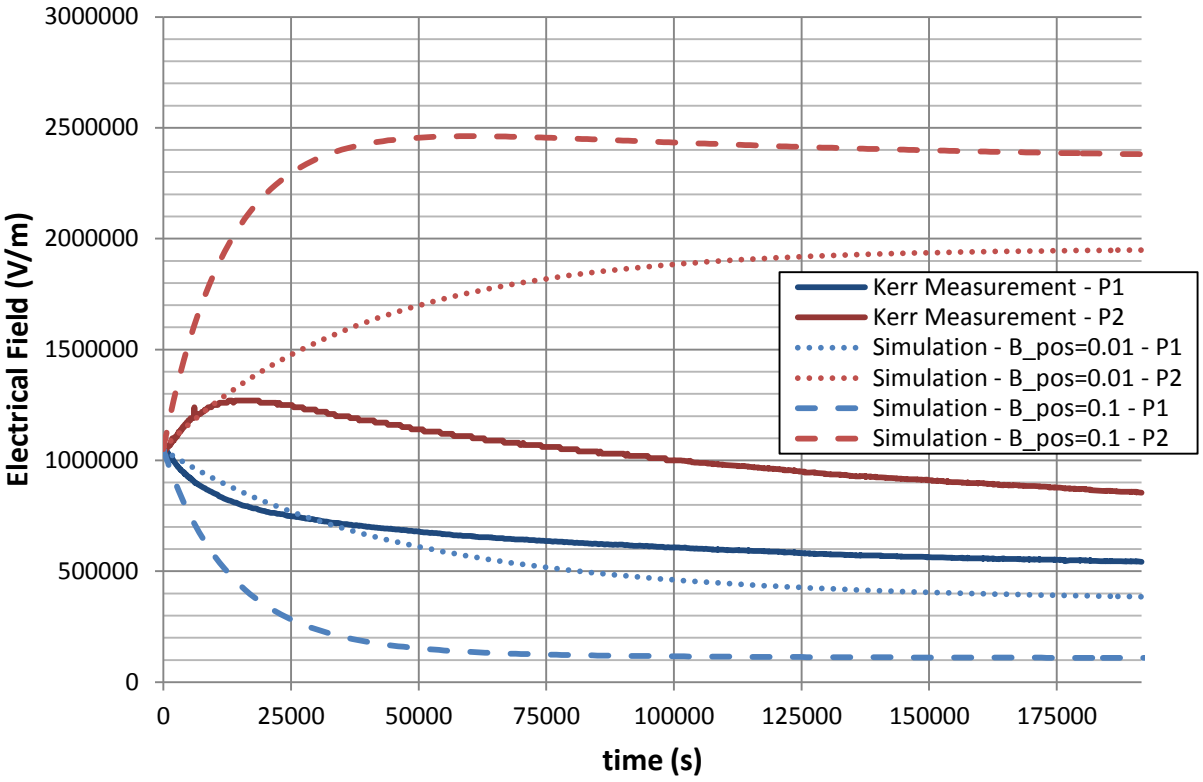

Figure 30. Case 2 +20kV: Simulation of ion drift diffusion model with positive injection from the oil-pressboard interface

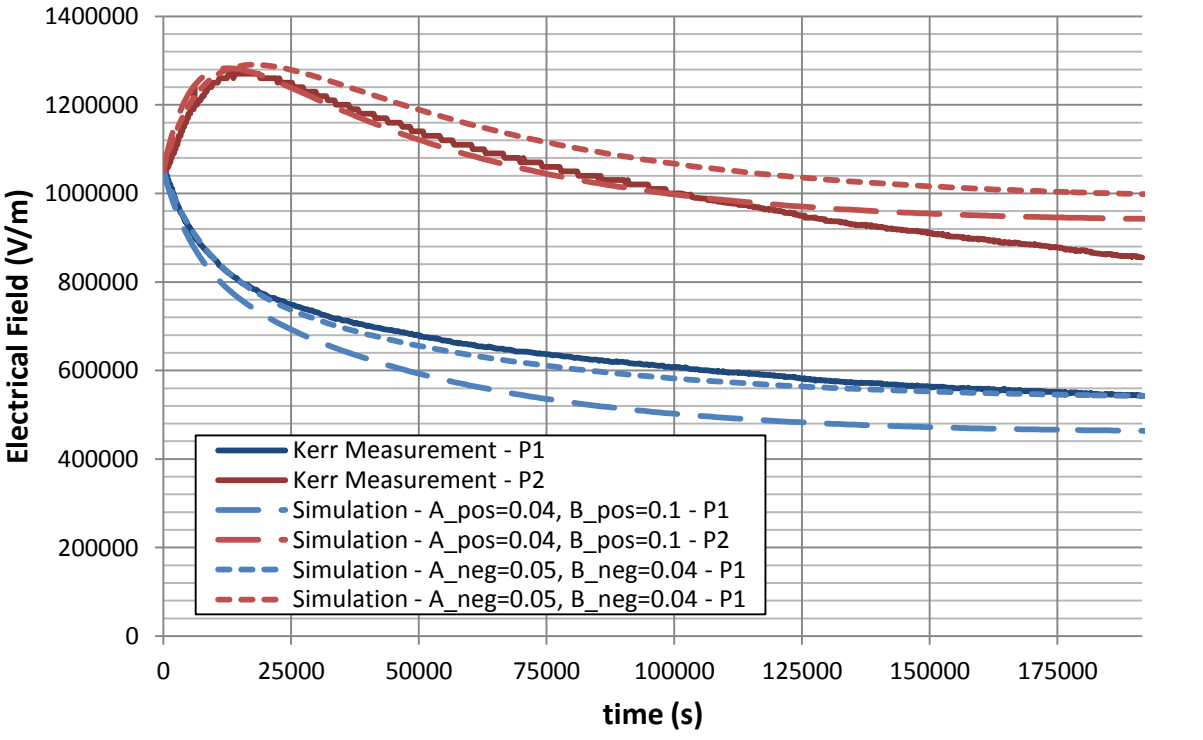

Figure 31. Case 2 +20kV: Simulation of Ion drift diffusion model with injection from the pressboard and the electrodes of the same sign.

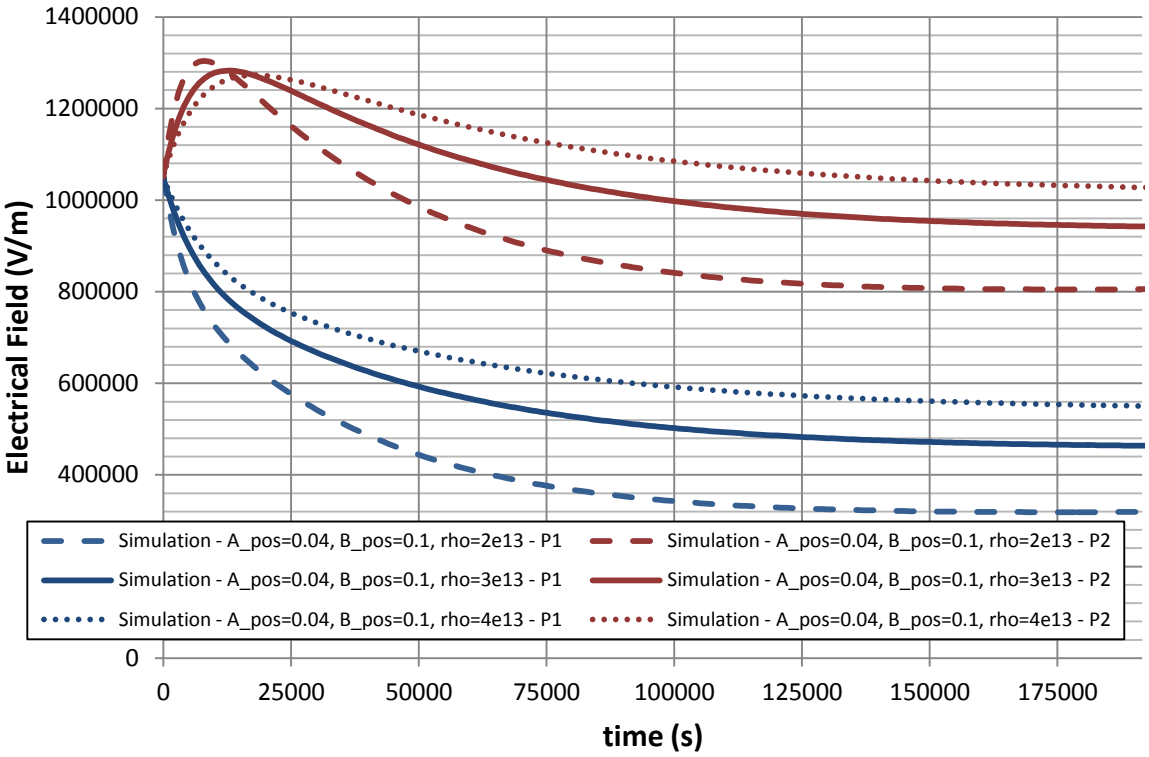

Figure 32. Case 2 +20kV: Comparing result of positive injection for different resistivities.

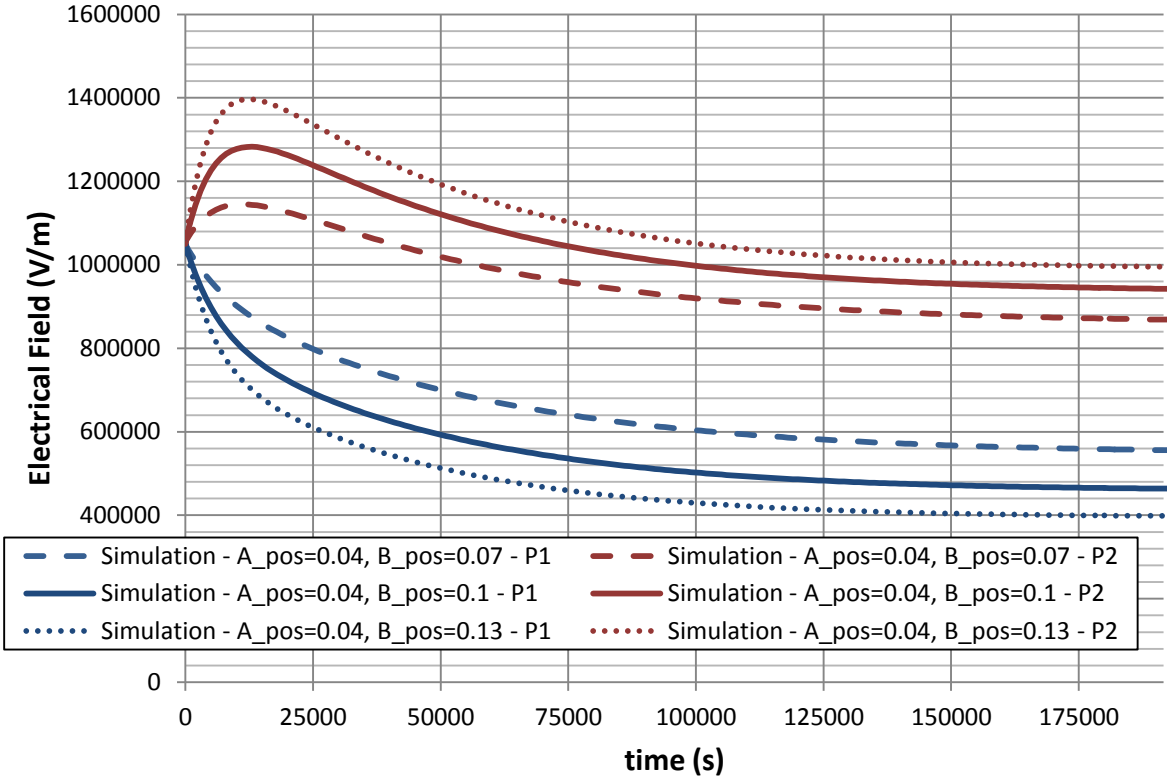

Figure 33. Case 2 +20kV: Sensitivity analysis for changes in B_{pos}. Here the parameters for the positive injection in Figure 31 as a starting point.

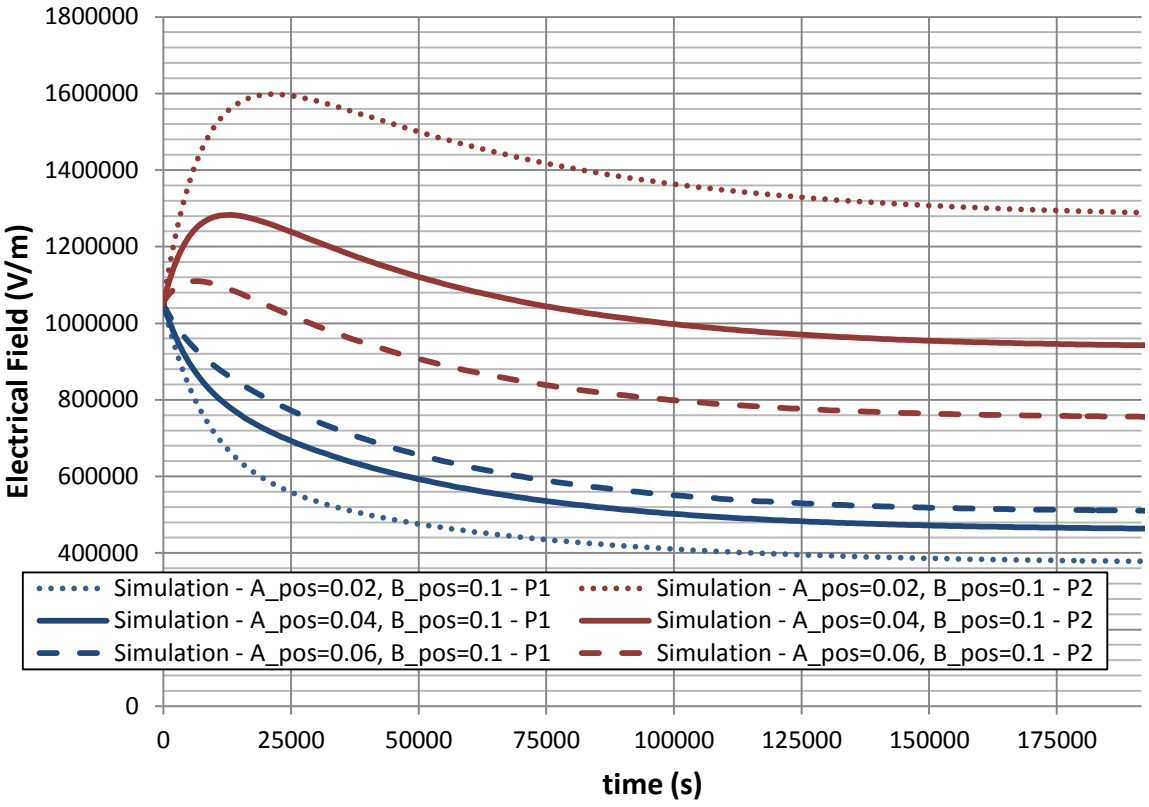

Figure 34. Case 2 +20kV: Sensitivity analysis for changes in A_{pos}. Here the parameters for the positive injection in Figure 31 as a starting point.

5.4 Case 3: Oil Gap with Pressboard Barriers in inhomogeneous Field

Studying Case 3 is started off by first looking at the positive application of 2kV on the upper electrode. Just as for Case 2, the ion drift diffusion model was first modeled with injection only from the pressboard or the electrodes. Using negative electrode injection or positive pressboard injection resulted in bringing the electric field curve in the direction of the measured curve. Positive electrode injection and negative pressboard injection on the other hand brought the simulated curve farther away from the measured one. The result for negative electrode injection and positive oil-pressboard injection for different injection strengths are shown in Figure 35 and Figure 36. It can be seen that using only one injection allows for a fair agreement to the measured data. In this case injection strength of around 0.4 gives a good match in both cases.

An investigation of how combining different injection types allows for a match for the measured curves now follows. Combing electrode and pressboard injection with different polarities allows for 4 different combinations. One of these combinations, namely positive electrode injection and negative pressboard injection, will move the simulated curve further away from the measured one. The reason for this is that the two combined injections one by one make the solution worse. Simulations with appropriately chosen injection parameters for the 3 remaining combinations are shown in Figure 37. We see that either using only positive or negative injection from the electrode and the oil-pressboard interfaces, gives the best match. This corresponds to an injection into both oil gaps.

The question is now how well these sets of injection parameters models the situation when -2kV is applied to the upper electrode. Negative electrode injection and positive pressboard injection is once again studied separately. The results are shown in Figure

38 and Figure 39. It can be observed that the curvature of the simulated curves does not quite match the measured one. This is especially not true for an injection strength of 0.4, which seemed to be a good parameter when applying +2kV.

Next up are simulations for the different combinations of injection parameters earlier used in Figure 37. They are presented in Figure 40. Just as before, using only positive or negative injection from the electrode and the oil-pressboard interfaces, gives the best result.

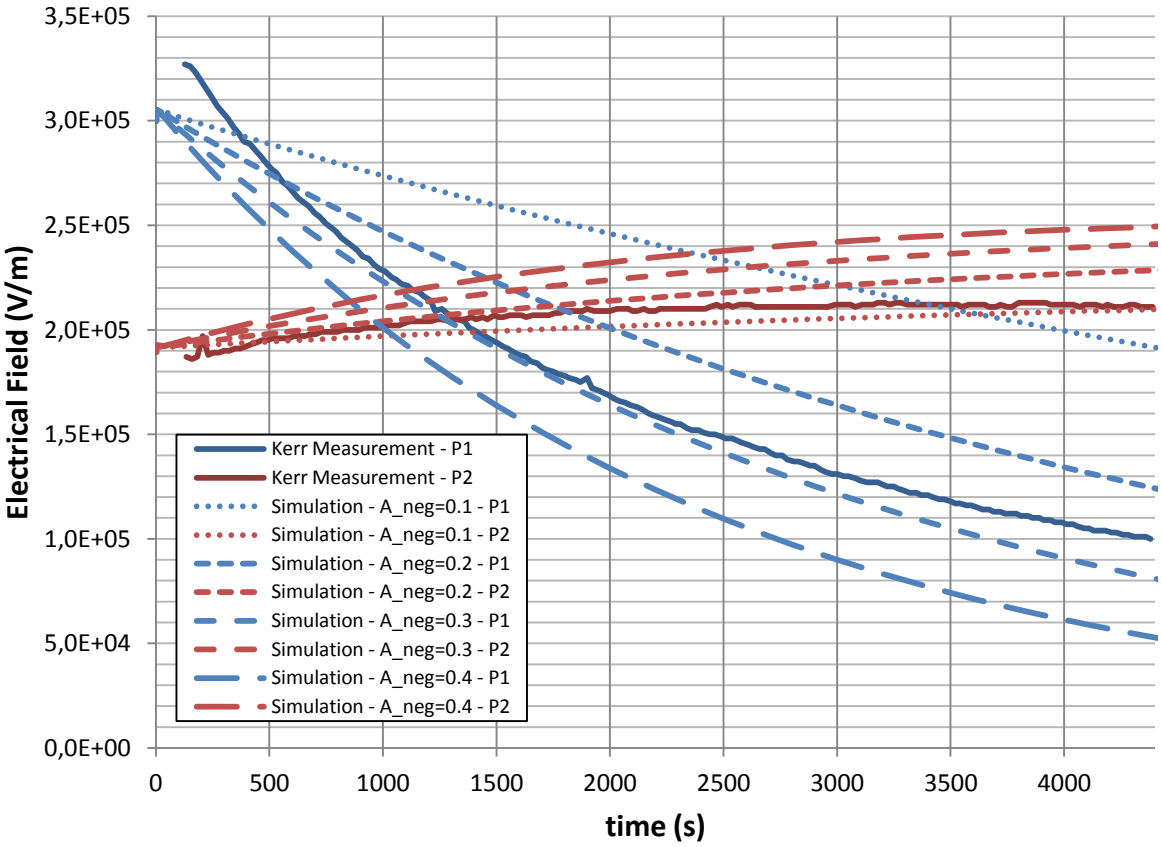

Figure 35. Case 3 +2kV: Simulation of ion drift diffusion model with negative injection from the electrodes

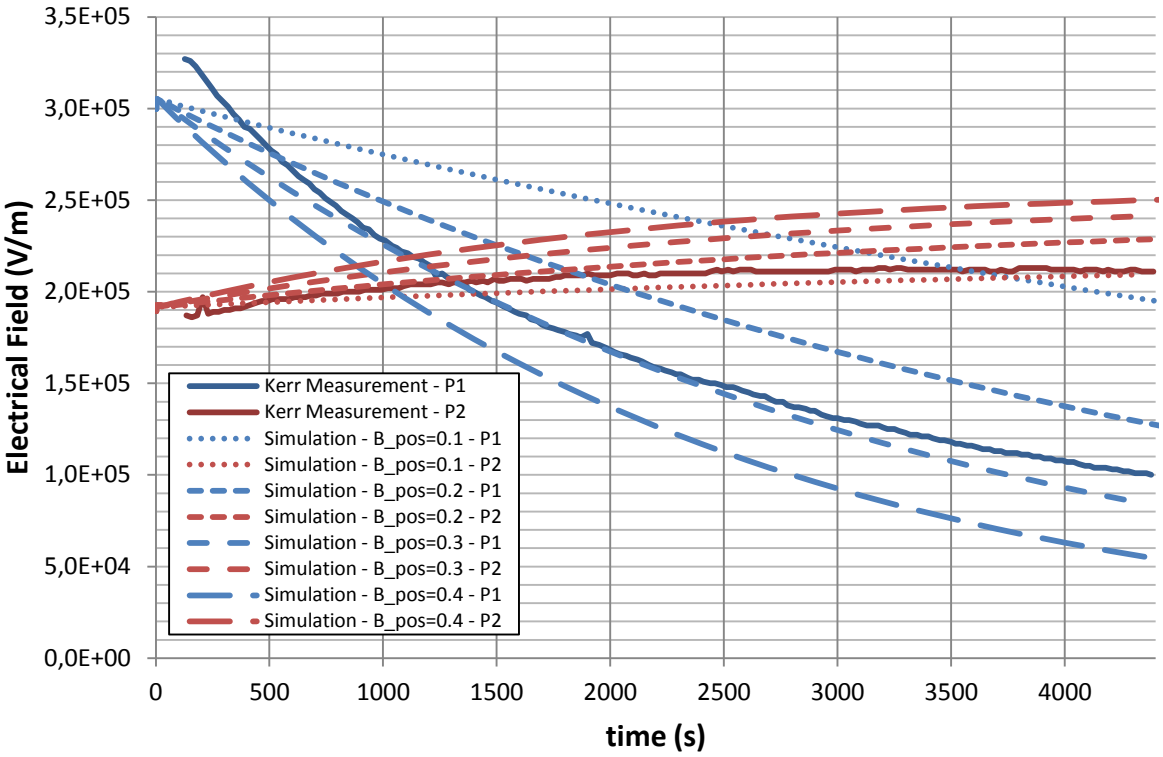

Figure 36. Case 3 +2kV: Simulation of ion drift diffusion model with positive injection from the oil-pressboard interface

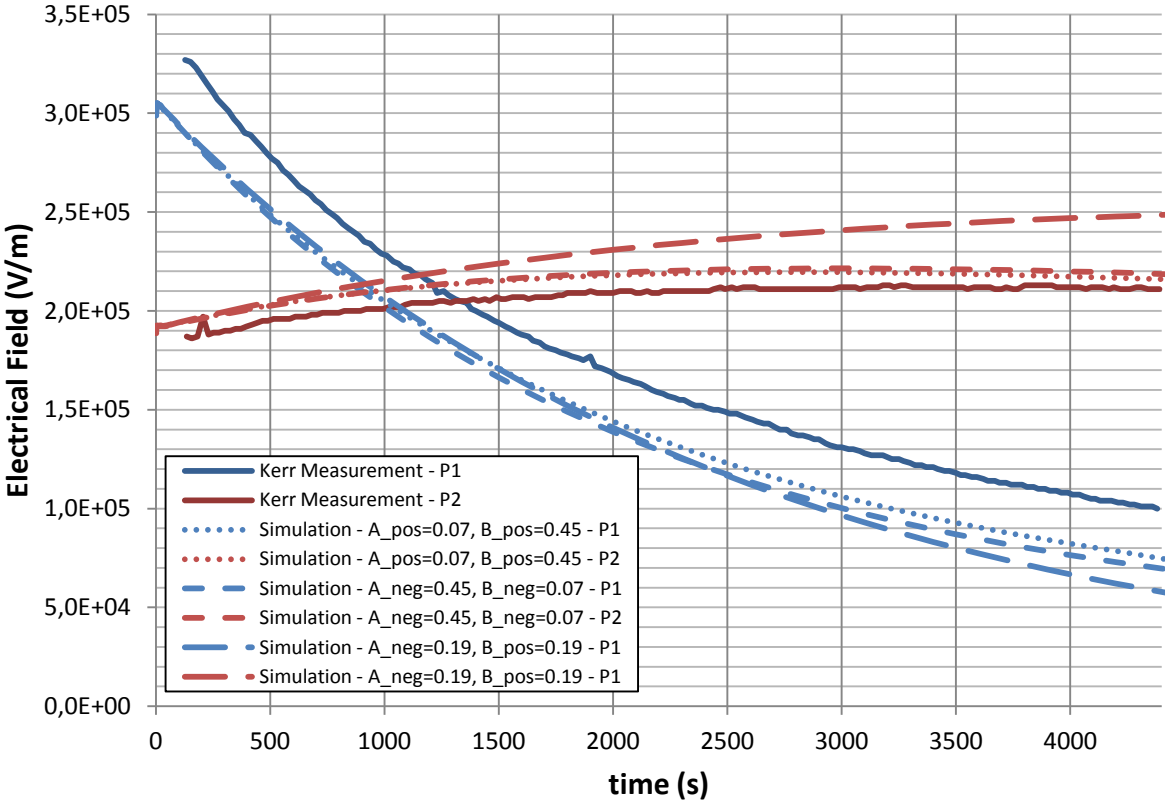

Figure 37. Case 3 +2kV: Simulation of ion drift diffusion model with combinations of electrode and pressboard injections that match Kerr measurements.

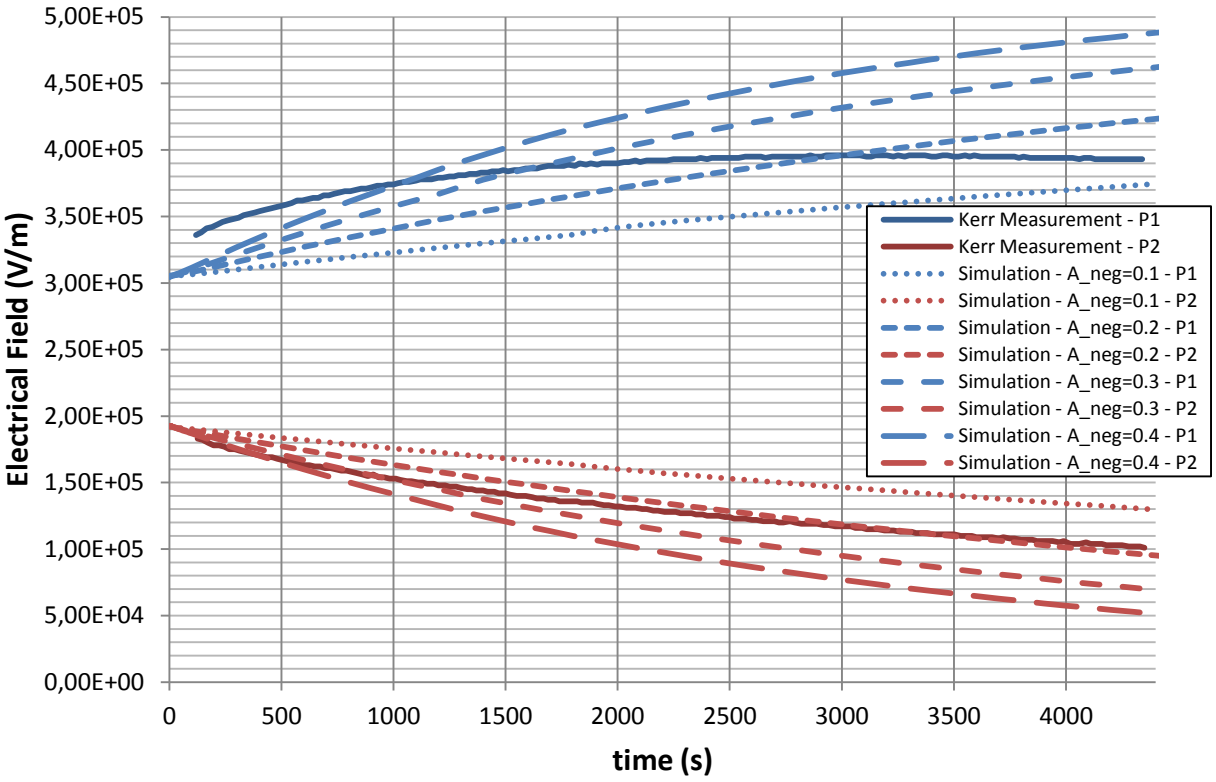

Figure 38. Case 3 -2kV: Simulation of ion drift diffusion model with negative injection from the electrodes

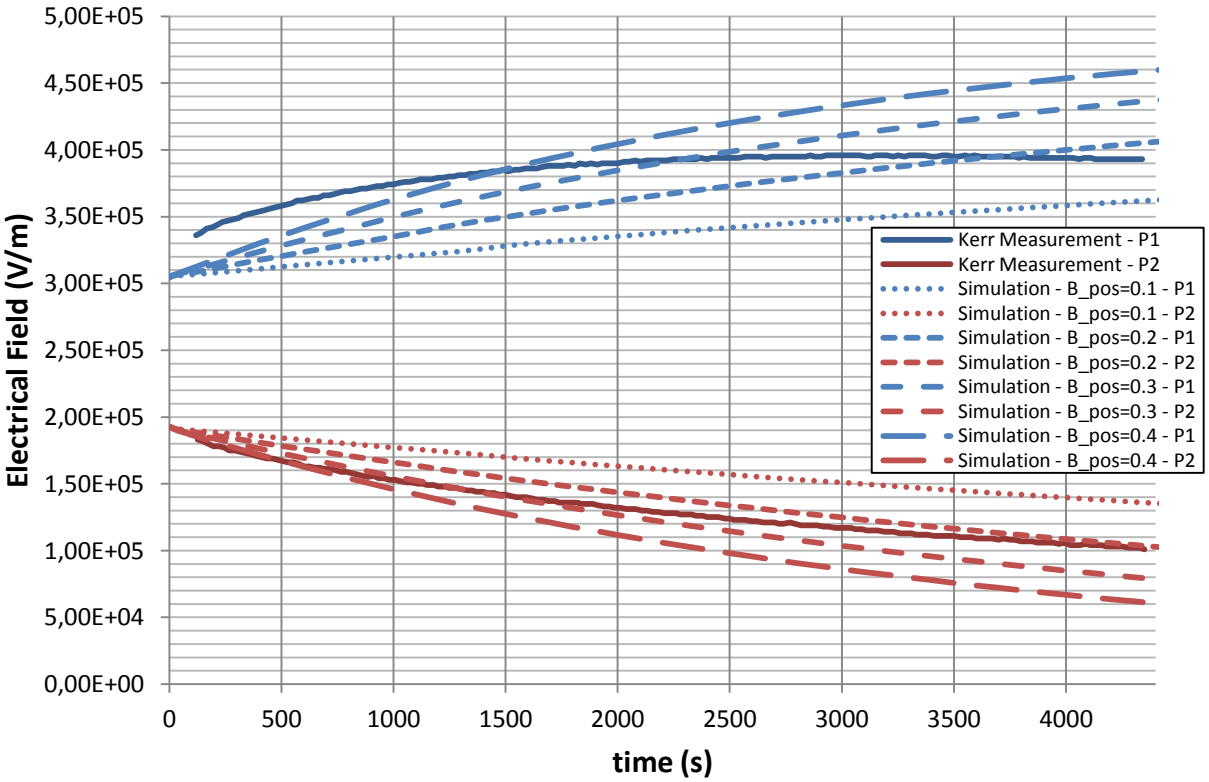

Figure 39. Case 3 -2kV: Simulation of ion drift diffusion model with positive injection from the oil-pressboard interface

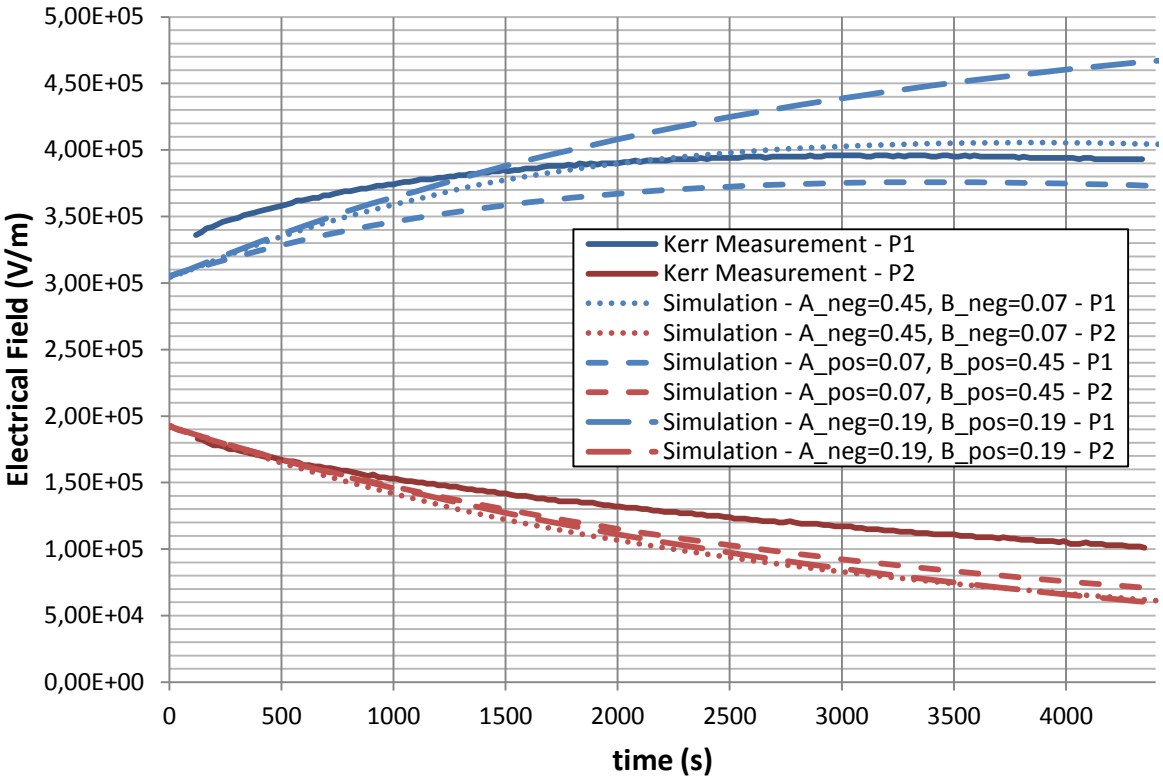

Figure 40. Case 3 -2kV: Simulation of ion drift diffusion model with the same combinations of electrode and pressboard injections as used for +2kV

5.5 Coaxial Test cell A and B

In order to better understand the measured currents for Coaxial Test Cell A and B, the results were compared with simulations with different conditions. To facilitate the comparisons between measured and simulated currents, only the magnitude of the currents was considered. To further facilitate the interpretation of the effect of the injection the terms inner and outer injection were introduced. Inner injection simply means that ions are injected from the inner electrode. This can be achieve in two ways in simulations, either by having the positive potential on the inner electrode together with a positive injection or by combining negative potential on the inner electrode with negative injection. Under the assumption that the positive and negative ion mobilities are equal, both these approaches yielded identical current magnitudes. Similarly, outer injection is when ions are injected from the outer electrode.

First to be studied was Coaxial Test Cell A using the Single Polarity Method. Here simulations were performed for inner and outer injection with different injection strengths. The results can be seen in Figure 41. Since the difference that arises from the use of inner and outer injection cannot explain the difference between the experimental currents, other explanations are sought. As mentioned before, the test cell was grounded for 3 days between the measurements. One idea is that the resistivity could have been altered somehow during this time. This possibility is studied in Figure 42 where the effects of different resistivities are compared.

The approach for the simulations of the Reversed Polarity Method was done in a similar way. Simulations were first made for inner and outer injection with different injection strengths. This is shown in Figure 43. First of all it is noticed that the current peak present in the measurements is not as well represented in the simulations. The reason behind this will be discussed later on. It can further be seen that the increase in injection

strength has several effects. First it increases the overall steady state current as well as the small difference in steady state current for inner and outer injection. Secondly it makes the transient currents for outer and inner injection differ more in curvature. In Figure 44 the study of Coaxial Test Cell A is finalized by a study of the effect of different resistivities. A higher resistivity will make the current peak larger as well as increasing the steady state current.

Finally simulations were performed for Coaxial Test Cell B, using the measured resistivity 2.4e13. Since the simulated steady state current was not in the same order of magnitude as the measured one, other resistivities were tried out. When using a resistivity around 2e12, a reasonable magnitude of the steady state current was attained. Even so, the shapes of the transients of the simulated and measured currents look nothing alike. With the purpose of getting a simulated transient current that was comparable with the measured one, the parameters of the injection was experimented with. However, this did not result in any considerable improvements of the simulated current. Simulations for the two resistivities mentioned above are shown together with the measured currents in Figure 45. Here the unipolar injection strength 0.3 is used.

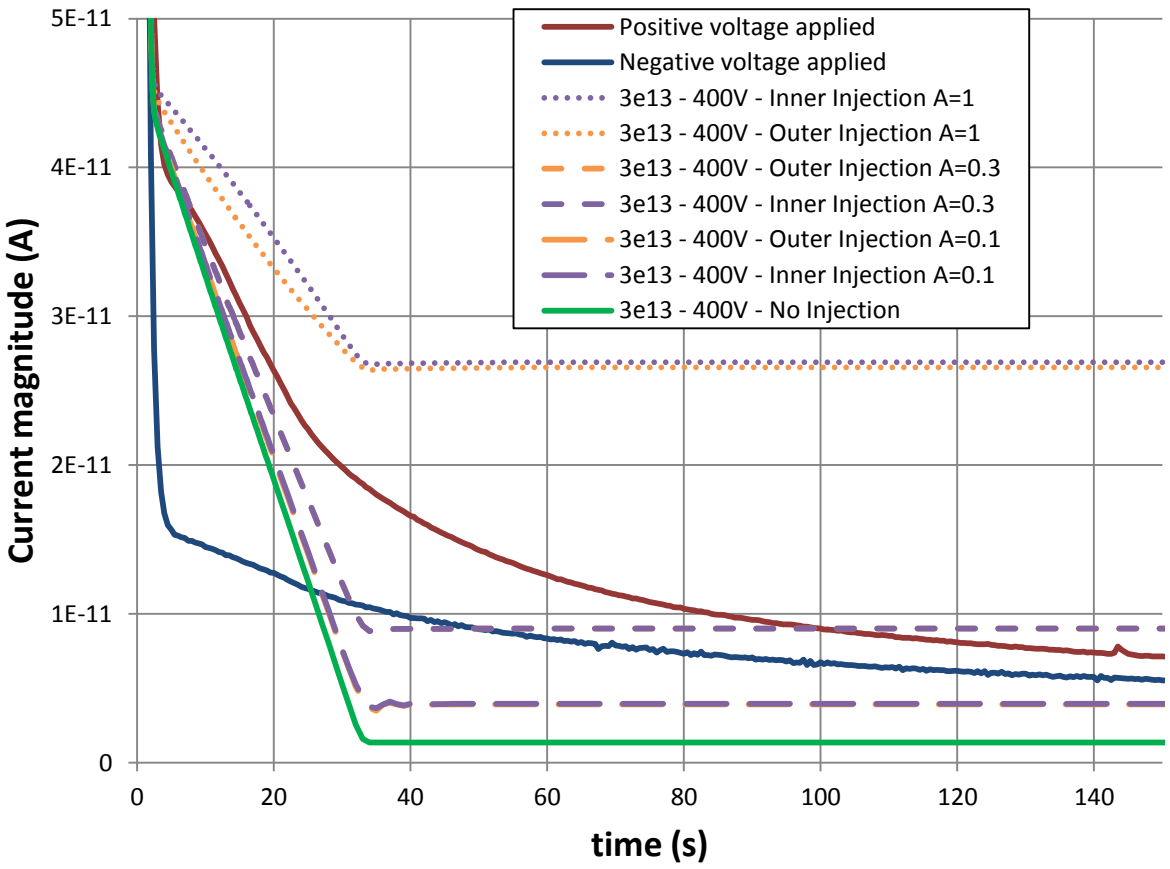

Figure 41. Coaxial Test Cell A – Single Polarity Method 400V: Simulated current curves with inner and outer injection of different strengths compared with measurements.

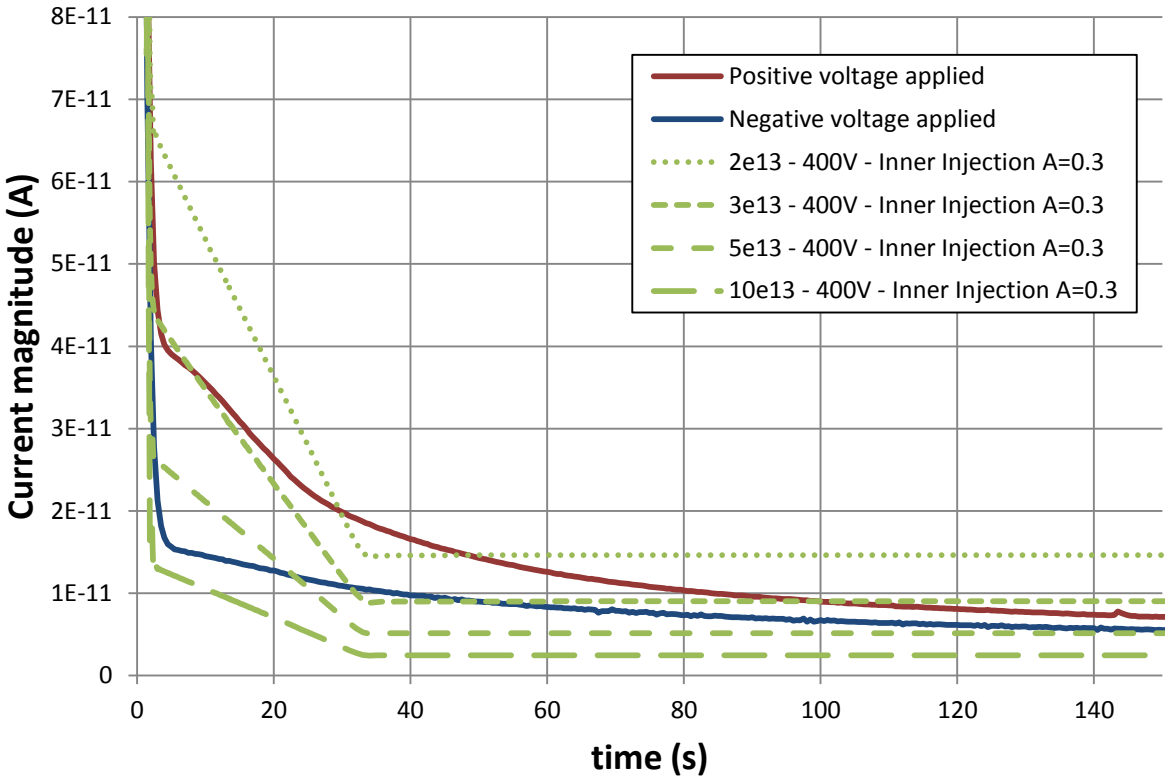

Figure 42. Coaxial Test Cell A – Single Polarity Method 400V: Simulated current curves for different resistivities compared with measurements.

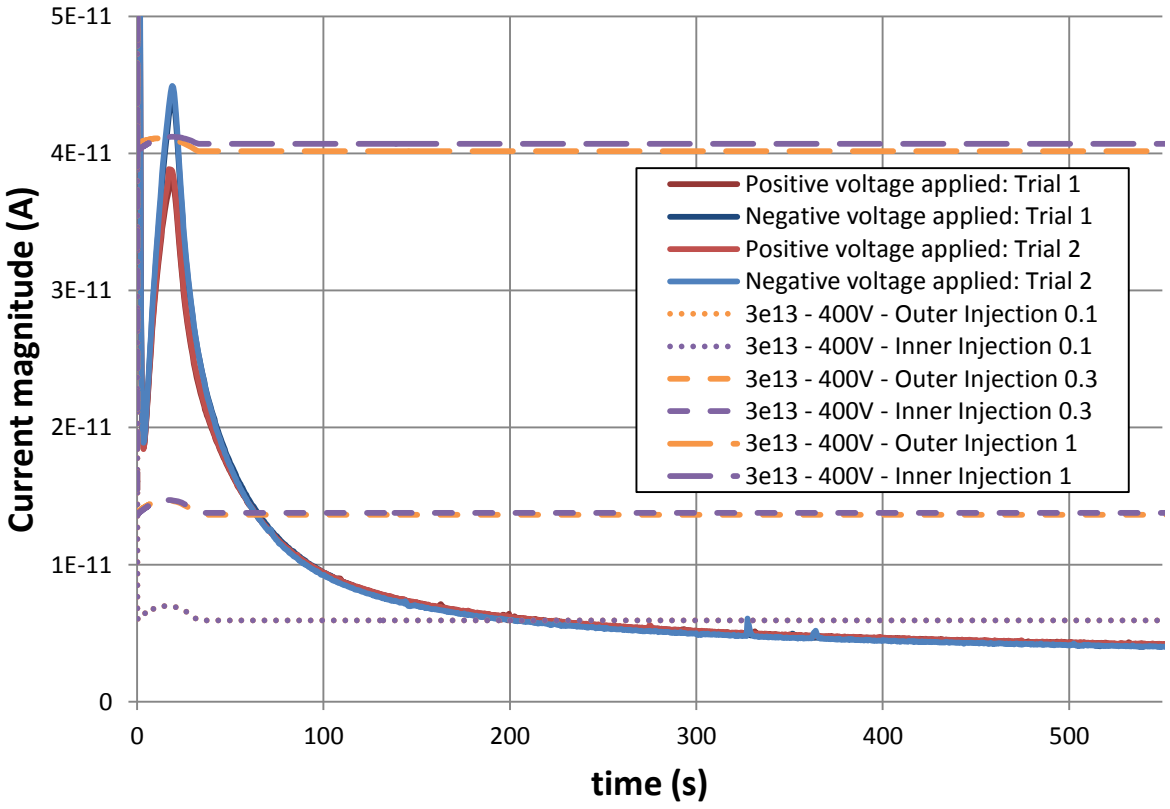

Figure 43. Coaxial Test Cell A – Reversed Polarity Method 400V: Simulated current curves with inner and outer injection of different strengths compared with measurements.

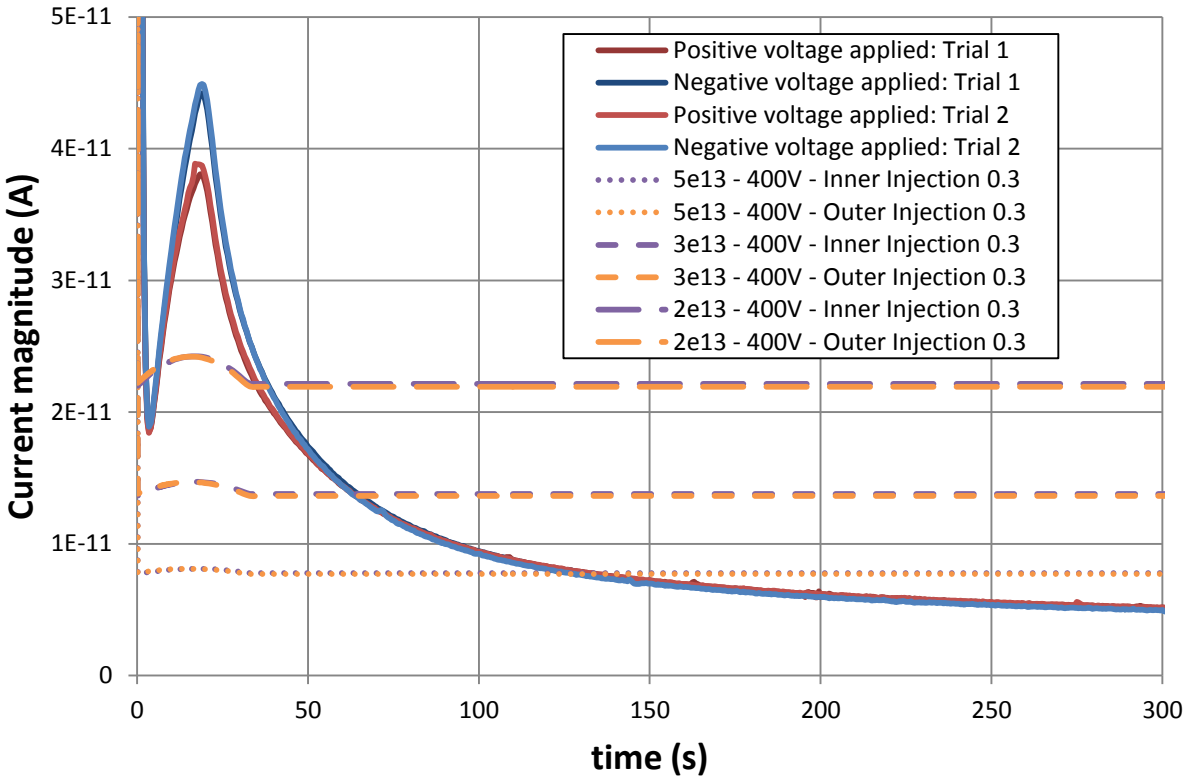

Figure 44. Coaxial Test Cell A – Reversed Polarity Method 400V: Simulated current curves for different resistivities compared with measurements.

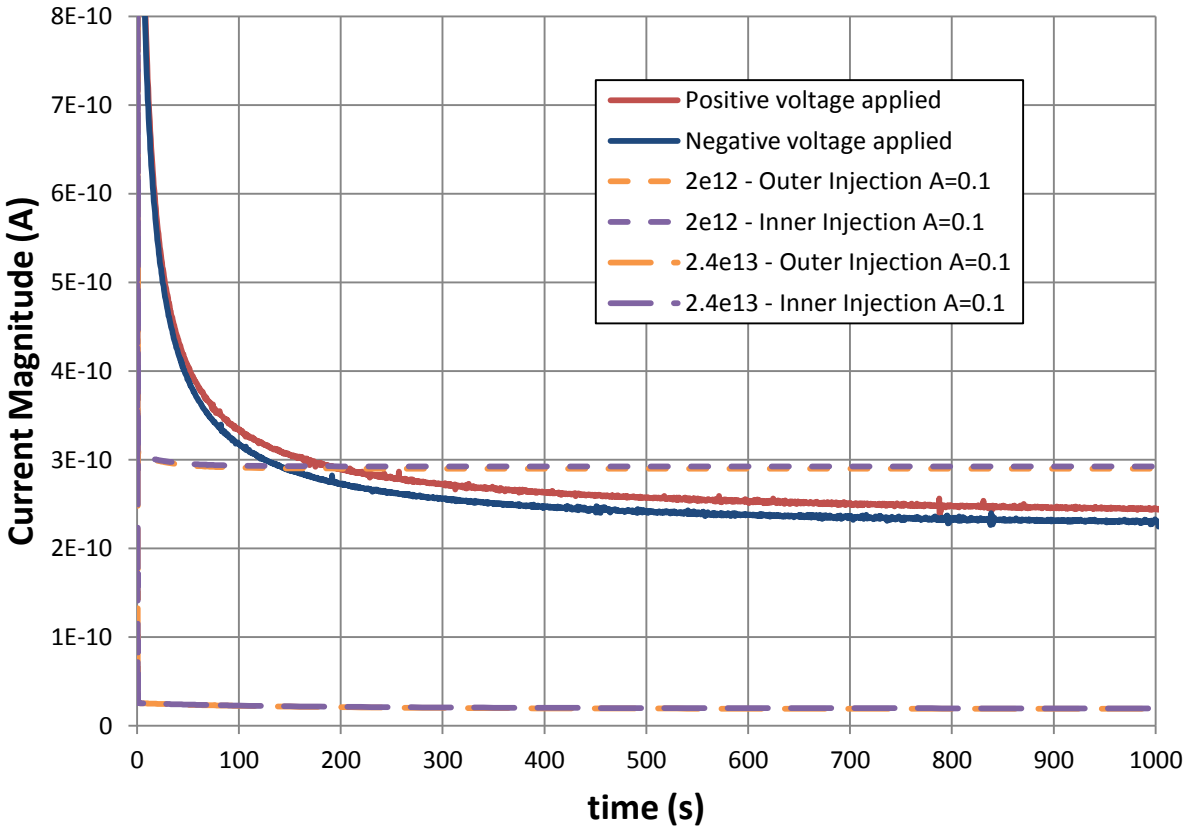

Figure 45. Coaxial Test Cell B – Single Polarity Method 1000V: Simulated current curves for two different resistivities compared with measurements.

6 DISCUSSION

6.1 Sources of Error of Importance

The transformer oil is very pure and hence contains a low amount of ions. That is why the resistivity of the oil is sensitive to impurities that for instance could be found in the test cells before the oil is added. A droplet of water is further enough to change the resistivity one order of magnitude.

When a measurement of the electric field or the external current is performed, the resistivity is usually measured before and after the experiment. That way it is possible to get an idea of how much the resistivity is varying. Normally this difference is of a significant size, indicating that there might be some reactions induced by the applied electric field that changes the resistivity.

Looking at the Single Polarity Method experiments for the Coaxial Test Cell A, it can be seen that there is a big difference in transient current, which through simulations only can be described by a difference in resistivity (See Figure 42). The difference is not as big for the Reversed Polarity Method. One important difference between the Single and Reversed polarity methods is that for the Single Polarity Method, the system has been grounded for 3 days between the measurements. This leads to the belief that there might be a slow reaction process that changes the resistivity throughout time.

The key point here is that the variations in resistivity complicates the study of the injection.

Kerr Measurement

The initial electric field distribution for any given geometry can be accurately calculated, since it is only dependent on the geometry of the system and the applied voltage. In the figures where simulations and measurements are compared for Case 3, a significant difference in the initial electric field can be observed. Such a difference is not observed for Case 2.

In Kerr measurements, sending beams of light through the test geometries allows for measurement of the birefringence being induced by the electric field. The spatial uncertainty of the measurement lies in the position in space where the measurement is done and at which angle the beam is sent. Optimally the beam would be sent in perpendicular to the cross section of the geometries. The uncertainty in position is not a big problem for Case 2 since the field is close to homogenous in the oil gap. For Case 3 on the other hand, a change in tenths of mm in the position of the measurement will yield different measured electric field strength. In Figure 46 we show how the electric field curve change when the position to the bottom electrode is altered with 0.3 mm.

Coaxial Test Cells

The Coaxial Test Cells were never completely filled why the exact height of the test geometry is unknown. Changing the height of the test cell will however only scale the magnitude of the currents and hence not affect the shape of the curve.

Simulations

Appropriate injection parameters were determined through trial and error. Since the whole parameter space have not been searched through it is likely that there are additional sets of parameters that yield a matching result as well.

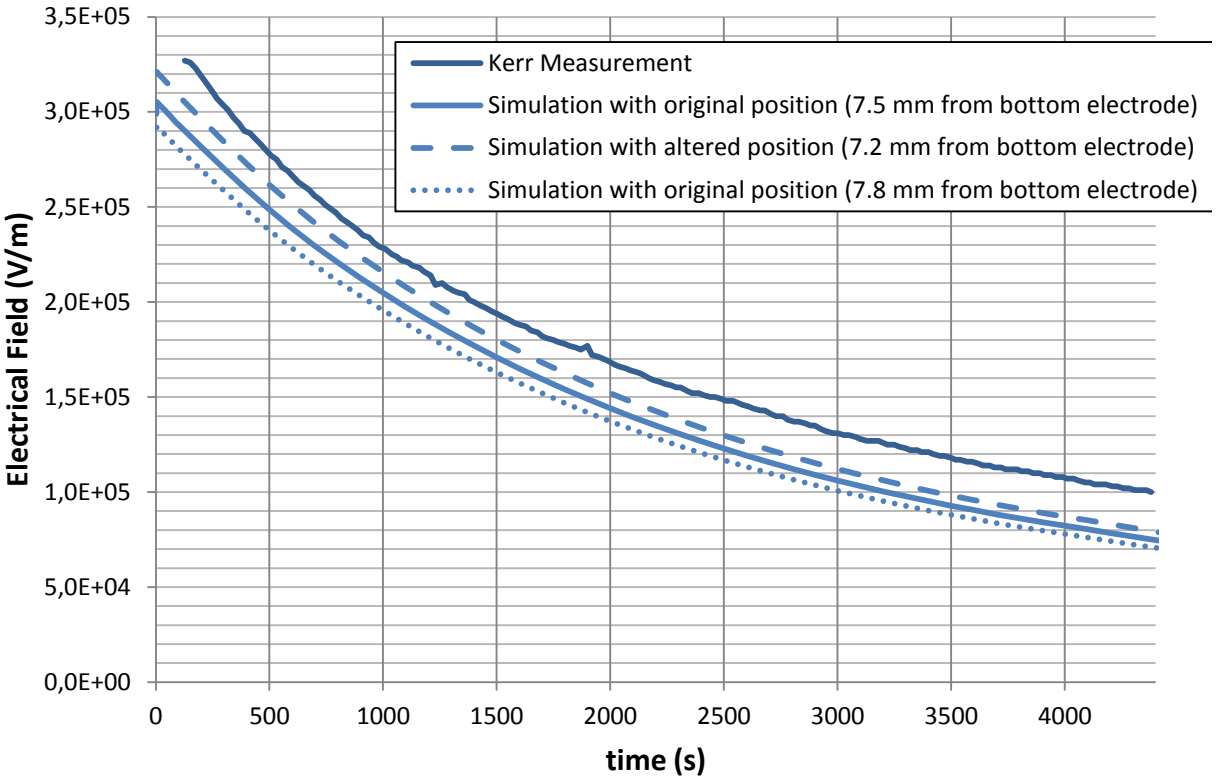

Figure 46. Case 3 +2kV: Simulations for point P1 with different offsets. Here A_{pos}=0.07 and B_{pos}=0.45

6.2 Sign and Strength of Injection in Blank Oil Gaps

When the Kerr measurements of Case 1 in Figure 10 is examined, it can be seen that the electric field has a parabola shape for low voltage and looks like a straight line for the higest voltage. When the ion drift diffusion model without injection is used to simulate the electric field, only parabola shapes can be attained. When a field independent ion injection is added to the model, it is possible to distort the parabola shape of the electric field. But the general shape of the electric field distribution will still remain the same when the applied field is changed. First when a field-enhanced injection is used it becomes possible to have different curvature for different voltages. The field enhancement is therefore essential to be able to match the result for different voltages with the same injection parameters.

To be able to draw the conclusion that the sign of the dominant injection is positive, it has to be clear that the distortion of the electric field really is due to the injection. One could argue that a difference in ion mobilities for positive and negative charges would yield an asymmetry of the electric field. But since the ion mobilities in the nearest are field independent, this does not go along with the field dependency observed for the distortion in the measurements. Earlier measurements further shows that there is no or a very small polarity dependence of the ion mobility [13]. Therefore the injection is assumedly dominated by positive injection.

The same Kerr measurements for Case 1 presented in Figure 10 have also been performed for the more resistive transformer oil used in Case 2 and 3. But since it contains much less free charges, the shape of the electric field could not be clearly determined. The measurement noise was simply too large to allow for distinguishing the shape. But this still remains an interesting experiment for the future, provided that the measurement noise can be decreased. The difference in resistivities between the oils

are due to the number of available free charges, but this is probably not the only difference. There might be chemical differences that effect the ion injection. The observation of positive injection should therefore not just be assumed for the more resistive oil.

Looking at the steady state current for Coaxial Test Cell A using the Reversed Polarity Method, a small but consistent difference can be seen between the different polarities. The steady state current for the positive voltage is found to be a little bigger and the same difference can be found in simulations between inner and outer injection. To be able to draw the conclusion that the injection is positive, the effect that a small difference in mobility has in a coaxial symmetry must be further studied.

In Figure 45, measurements and simulations for Coaxial Test Cell B were compared. When using the measured resistivity for the simulations, the steady state current was deviating from the measured one by an order of magnitude. What was also observed was that the shapes of the measured and simulated curves were not comparable. Since we do not understand why simulations and measurement are that different, we cannot draw any conclusions about the ion injection for that case.

The question is now weather it is possible to draw any conclusions about the apparent injection strength. For the data of Case 1, assuming unipolar injection, the injection strength was estimated to around 0.3. Imagining the injection to be bipolar allows for a variation of the positive and negative apparent injection strength while still maintaining a difference of 0.3. In Figure 47 and Figure 48 the electric field is simulated for different values of positive and negative injection, restricting their difference to be 0.3. From Figure 47 we see that the largest injection strength ($A_{pos} = 0.7$, $A_{neg} = 1$) yields an electric field distribution that is completely wrong. Setting the injection strengths in the interval $0 \leq A_{neg} \leq 0.3$ and $0.3 \leq A_{pos} \leq 0.6$ gives results very much comparable to using a unipolar positive injection strength of 0.3.

6.3 Sign and Strength of Injection in Oil-Pressboard Systems

Without considering bipolar injection, Case 2 shows that the pressboard injection must have the same sign as the electrode injection for measured and simulated data to match. But if a bipolar injection is allowed, no such conclusion can be drawn. In Figure 49, a few possibilities of bipolar injection that allows for a match for Case 2 are shown. What however can be said for the injection in general is that there must be an injection in both oil gaps in Case 2 in order to allow for an agreement with the experimental data. This is also true for Case 3, although the much shorter measurement times does not allow for a conclusion as strong. For Case 3 it is further observed that injection in the lower oil gap for +2kV must be much larger in order to get the large drop in electric field strength found in the measurements.

Due to all the possible combinations of injection that can be put together to match the measurements of Case 2 and 3, no conclusion can be drawn about the sign of the dominant injection from the oil-pressboard interface.

Drawing a conclusion about the injection strength from the oil-pressboard interface is even more complicated. If the strength of the injection parameters needed for a fit is compared when using the same set of injection for Case 2 and 3, we observe a considerable difference. The difference is also larger for the oil-pressboard injection strength. Since the pressboard consist of cellusloe fibers whose structure is very complex and varying and also dependent on the production process, it might be that the difference in injection strength is due a difference in the structure of the pressboard.

Looking at the range of the values of the injection parameters that gave a good fit to experiments, it can however be assumed the injection strengths lies within the range 0.01 to 1.

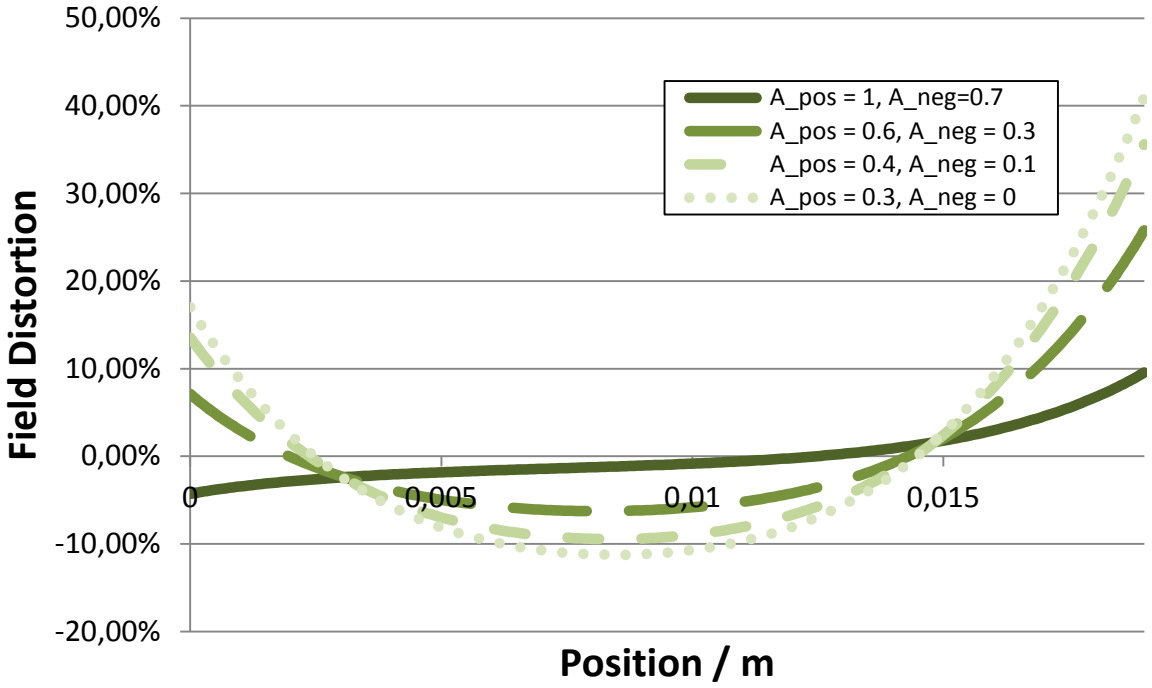

Figure 47. Case 1 with 2kV applied: Steady state electric field for different injection strength where $A_{pos} - A_{neg} = 0.3$. The resistivity of the oil is $2 \cdot 10^{12}\ \Omega m$

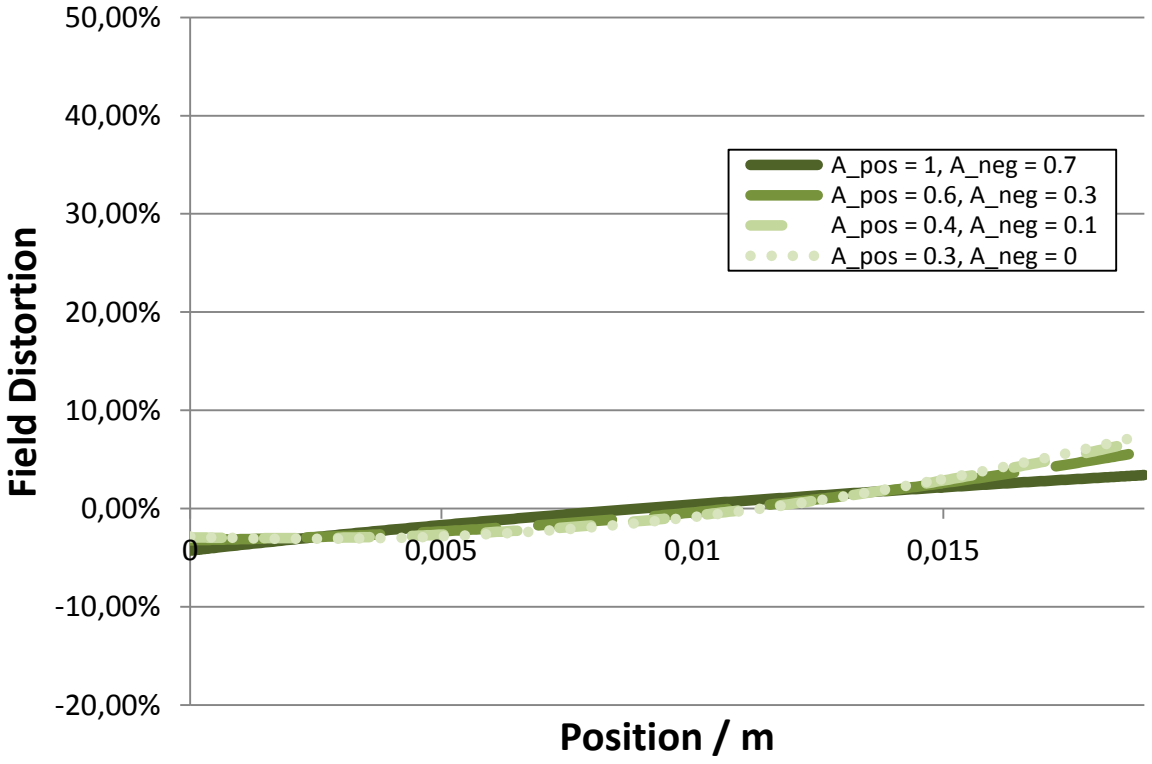

Figure 48. Case 1 with 20kV applied: Steady state electric field for different injection strength where $A_{pos} - A_{neg} = 0.3$. The resistivity of the oil is $2 \cdot 10^{12}\ \Omega m$

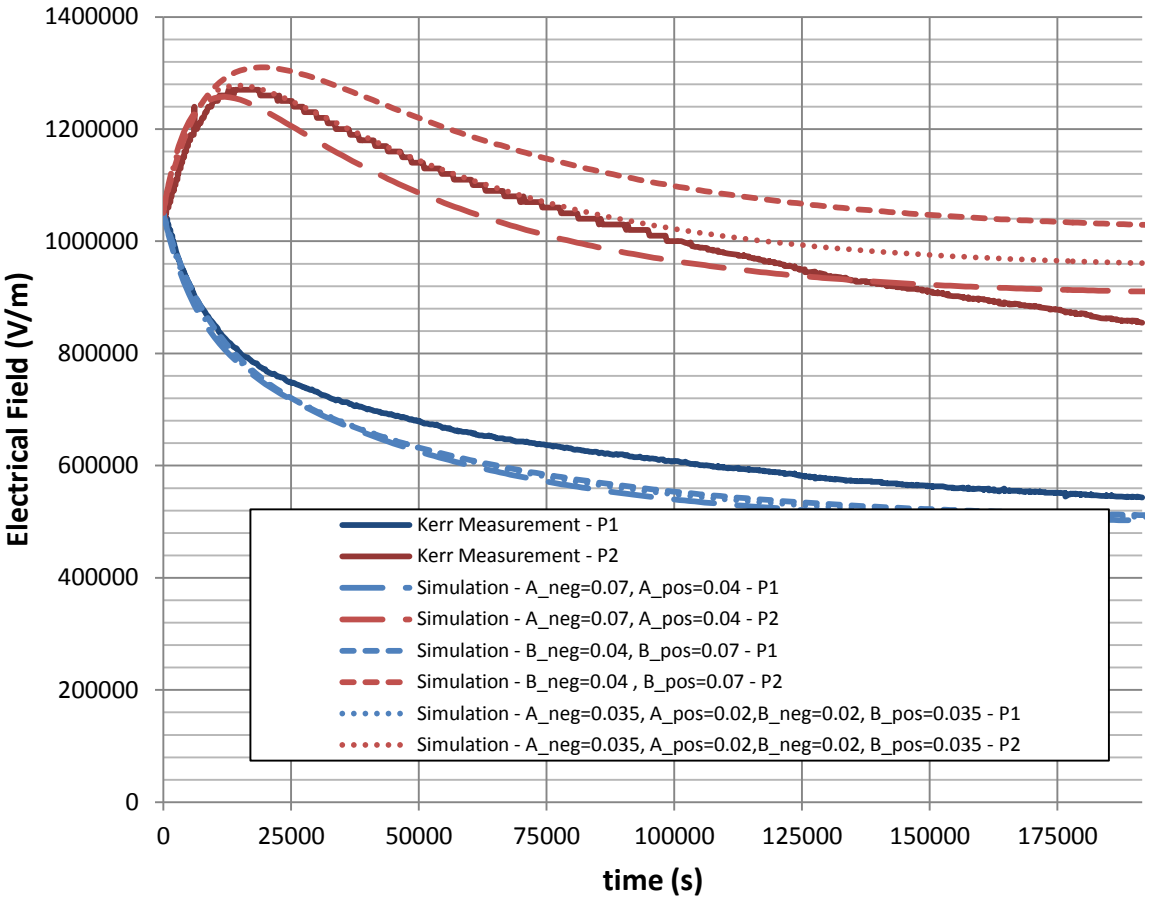

Figure 49. Case 2 +20kV: Simulation of ion drift diffusion model with bipolar injection

6.4 Possible improvements of the ion injection model

The field enhancement of the ion injection from the oil-pressboard interface is modeled with a dielectric constant of the pressboard of 4.2. The dielectric constant for the oil-impregnated pressboard is an average of the dielectric constants in oil and in pressboard. The dielectric constant for the cellulose fibers in the pressboard is normally around 6, and it might be more correct to use a value like that when calculating the effective permittivity for the field enhancement. After all, on the microscopic level it is an interface between cellulose fibers and oil. The pressboard being oil-impregnated means that all cavities in the pressboard are filled with oil, and this shouldn't have any effect on the interface. How the field enhancement is altered when 6 instead is used as the dielectric constant for pressboard in the effective permittivity is shown in Figure 50.

For the field enhancement it has also been assumed that the field at the interface is equal to the field in the oil just outside of the interface. In reality the pressboard interface will consist of a lot of sprawling fibers. Being seen as protrusions these fibers would give rise to a local enhancement of the field, which should be taken into account for the injection. The effect of a locally enhanced field on the field enhancement of the ion injection is simulated in Figure 51. Depending on the size of the local enhancement, the field enhancement of the injection could be considerably increased.

The surface of the pressboard is further folded, which means that the effective surface of the interface is larger than the cross section area. This could give rise to larger injection and would practically implicate a larger value of the injection strength parameters B_{pos} and B_{neg}.

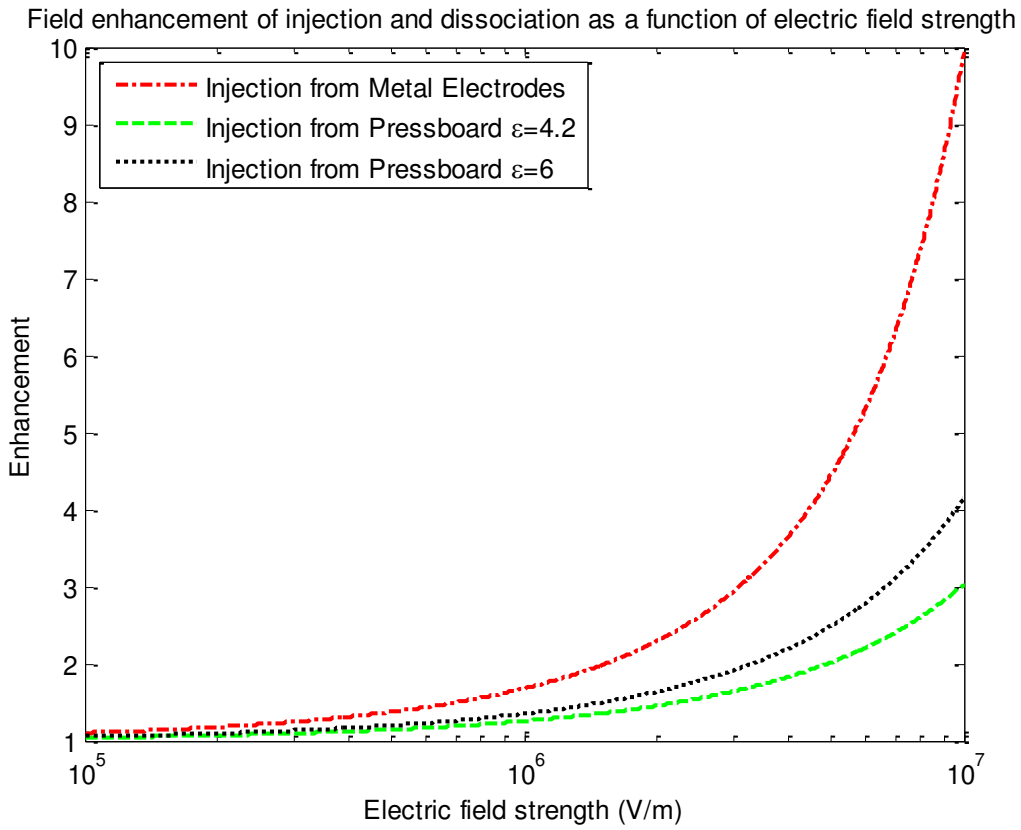

Figure 50. How the field enhancement of the injection from the pressboard/oil interface is dependent on adjustments of the effective permittivity.

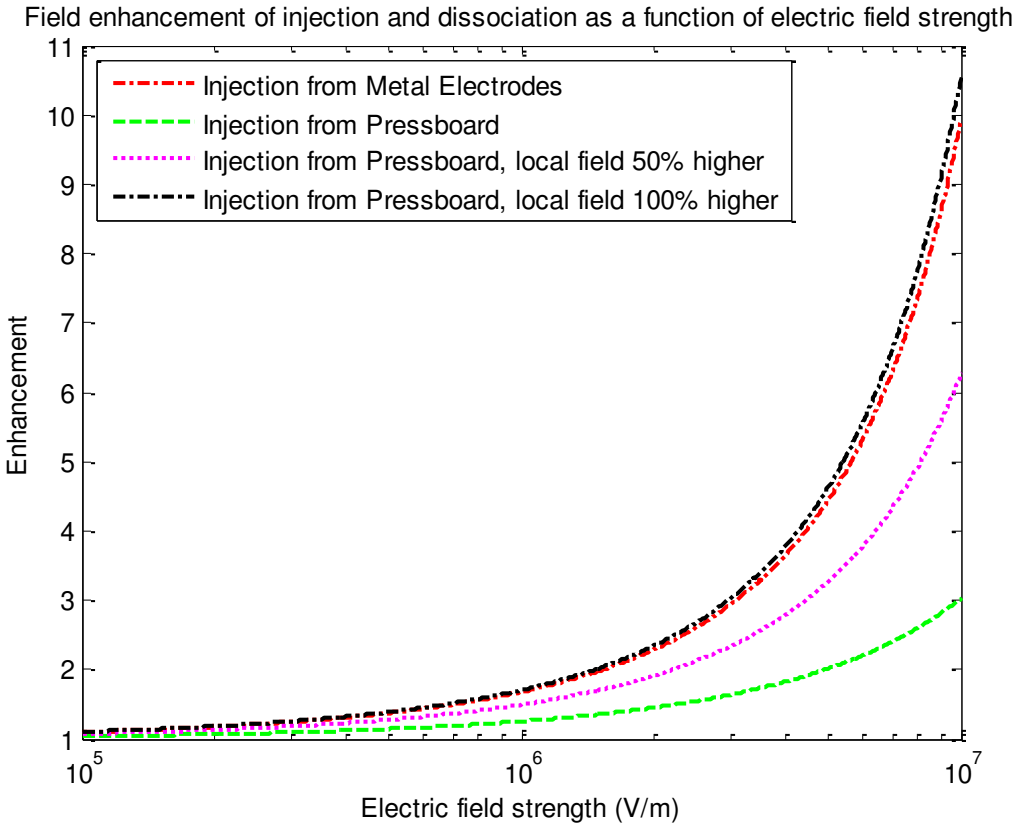

Figure 51. How the field enhancement of the injection from the pressboard/oil interface is affected by local field enhancements.

When studying the results of the Reversed Polarity Method for Coaxial Test Cell A in Figure 43, it was seen that the current peak in the experiments was much larger than that in the simulations. The reason for this could be that the way the external boundaries are modeled is incorrect. In reality ions that reach the electrodes would take part in a charge transfer reaction. What is done in simulations is that ions are being transferred out of the system directly as they reached the contacts, which is equivalent to the charge transfer reaction occurring instantly. If this is not the case there will be a bigger buildup of charges then predicted by the simulations. When reversing the polarity, this would then give rise to a bigger current peak.

For all the current measurements for the coaxial geometries, there is a slow transient that make the current slowly decrease over time. The reason behind this behavior is not understood and should to be further investigated in order to improve the modeling. Further comparing the measurements and simulations for Coaxial Test Cell B, a big difference for the first seconds of the transient current is seen. A first reaction to this effect was that it was due to a slow onset of the applied voltage. But the onset time was determined by measurements to be in the order of milliseconds. One idea is that the injection is time dependent, and that the diffuse layer is being swept out the first seconds. This would be an explanation for an initially strong injection that passes over to a weak injection. The existence of a time dependent injection should be further investigated to understand the measurements of the Coaxial Test Cell B.

It has been shown that the ion drift diffusion model can be used to accurately estimate the electric field in oil [1]. It is however important to notice that the types of ions present in the oil are unknown. The mobility for positive and negative ions has been measured, but this does not mean that the existence of only one kind of ion for every polarity has been proven. The measured mobility could be an effective average of the mobility of all the ions in the oils. If there are several types of ions present in the oil, the recombination and generation process would be much more complicated than currently modeled by the ion drift diffusion model. It is further assumed that the ion pairs consist of one ion of each polarity. Finally it is also assumed that the injected ions are of the same type as those in the bulk of the oil. Therefore they would able to react with each other. Whether or not these assumptions are good remains an important question. This question should be resolved in the future by investigating the present ions in the oil and what their properties are.

6.5 Single Polarity Method versus Reversed Polarity Method

When the Single Polarity Method is used the initial state of the system is clearly defined. The initial concentration of ions in the oil is given by the resistivity of the oil. However, to be sure that the initial state has been reached, the test cell must be grounded for quite some time. It seems like the resistivity is changed a considerable amount during this time, why it is problematic to compare the measurements for different polarities.

The advantage of the Reversed Polarity Method is that the time between the measurements for the different polarities is much shorter. It can therefore be assumed that the resistivity is the same for the different measurements. However, as of now the initial conditions for this method is not correctly modeled. By better understanding the interaction between the ions and electrodes, the boundary conditions of the system could be better modeled. If this would be achieve it could be possible to draw sharp conclusions about the ion injection from the Coaxial Test Cells.

7 CONCLUSIONS

A model for ion injection in oil-pressboard insulation systems has been implemented in the ion drift diffusion model. The ion injection model contained apparent injection from electrodes as well as from oil-pressboard interfaces. The validation against different test geometries showed that, with the right parameters, the ion injection model substantially improved the result of the ion drift diffusion model. Narrowing down the values of the injection strength parameters however proved difficult due to the big uncertainty in the resistivity of the oil. Conclusions specific to the type of test geometry used now follows.

Injection in Oil Insulation Systems

- For the low resistive oil used in [1], the injection from electrodes into oil was dominated by positive injection. The positive injection was found to be in the range 0.3-0.6 while the negative was in in the range 0-0.3. The difference between the injection strengths was found to be 0.3.
- The field enhancement of the injection is crucial in order to correctly model the electric field distribution for different electric field strengths.
- Using the Single Polarity Method to draw conclusions about the injection requires reducing the variations in the resistivity.
- Current measurements indicate that our model gives rise to an insufficient buildup of charges in the Reversed Polarity Method. This appears to be due to an inadequate modeling of the charge transfer reactions at the electrodes. A conclusion about the dominant injection sign from the distinct polarity dependence of the current measurements can only be done when the current peaks have been correctly modeled.

Injection in Oil-pressboard Insulation Systems

- It was found that multiple assumptions about the polarity (unipolar or bipolar) and the interfaces the injection was coming from (electrode or oil-pressboard or both) led to a fair agreement with the experimental data. This finding calls for further investigation in order to determine the set of injections parameters that conforms to reality.
- No conclusion could be made for the dominating sign of injection. To achieve simulation results matching the measurements, the injection strength parameters had to be set in the range 0.01 to 1.
- For Case 2, injection was needed in both oil gaps in order to get a match with the experimental data. Case 3 pointed in the same direction, but since these experiments were performed for a much shorter time, the observation was not as clear here.
- To describe the strong polarity dependence in Case 3, the negative electrode injection and the positive oil-pressboard injection together had to be considerably stronger than the positive electrode injection together with the negative oil-pressboard injection.

8 FUTURE WORK

It has been proven that the ion injection model improves the ion drift diffusion model. Now it remains to nail down the injection parameters of the model. This should be done through continued validation against experimental data. To facilitate the validation, some

question marks should also be cleared up. The following tasks are suggestions on what should be carried out in the future.

- The electric field measurements for Case 1 with the high resistive oil were too noisy to be able to draw any conclusion about the injection. These experiments should therefore be repeated in order to reduce the noise. That way a sharp conclusion about the ion injection strength and polarity dependence in high resistive oil could maybe be made as well.
- Using an altered Case 1 geometry could simplify the study of the apparent injection from oil-pressboard interfaces. By covering the electrodes with pressboard coatings, the same procedure used for determining the dominant injection sign for apparent electrode injection in Case 1 could be used.
- A detailed description of the charge reaction at the electrodes should be developed. This would improve the interpretation of the measurements using the Reversed Polarity Method. A partially blocking boundary condition for the ions could be developed to try to get a better match with the measured currents.
- The Kerr measurement for Case 3 was done for a very short time compared to Case 2. If the measurement were repeated for a longer time, then maybe additional parameter combinations could be excluded.
- The ion content in the oil should be determined somehow in order know whether the assumptions about the reaction mechanisms are fully valid.
- The slow decreasing transient behavior of the current measurements has to be investigated and understood so that the interpretation of the polarity dependency becomes easier.
- A deeper study of the field enhancement of the injection has to be done. For the oil-pressboard injection, there are several possible adjustments of the field enhancement that should be tested.

9 REFERENCES

[1] U. Gäfvert, A. Jaksts, C. Törnkvist and L. Walfridsson, “Electrical Field Distribution in Transformer Oil”, IEEE Transaction on Electrical Insulation, Vol. 27, No. 3, pp. 647-660, 1992.

[2] A. Denat, “Étude de la Conduction Electrique dans les Solvants Non Polaires”, Thesis L’Université Scientifique et Médicale et L’Institute National Polytechnique de Grenoble, 1982

[3] P. Langevin, “Recombinaison et mobilités des ions dans les gaz”, Annales de Chimie et de Physique, 28(7):433, April 1903

[4] L. Onsager, “Deviations from Ohm’s Law in Weak Electrolytes”, Journal of Chemical Physics, Vol. 2, pp. 599-615, 1934.

[5] A. Castellanos and F. Pontiga, “Generalized Thomson-Onsager model for charge injection into dielectric liquids”, CEIDP Annual Report, 22-25 Oct., 1995, pp.616-620.

[6] A. Denat, “Conduction and Breakdown Initiation in Dielectric Liquids”, IEEE International Conference on Dielectric Liquids, 2011

[7] M. Nemamch, J.P. Gosse,B. Gosse and A. Denat, “Influence of Insulating Electrode Coatings on the Electrical Conduction of Cyclohexane”, IEEE Transactions on Electrical Insulation, Vol. 23, No. 4, pp. 529-534, 1988.

[8] M.Nemamcha. J. P. Gosse, A. Denat and B. Gosse, ”Temperature Dependence of Ion Injection by Metallic Electrodes into Non-Polar Dielectric Liquids”, IEEE Transaction on Electrical Insulation, Vol. EI-22, No 4, pp. 459-465, August 1987.

[9] F. Pontiga and A. Castellanos, “Electrical Conduction of Electrolyte Solutions in Nonpolar Liquids”, IEEE Transaction on Industry Applications, Vol 32, No. 4, pp. 816-824, 1996.

[10] A. Denat, B. Gosse and J. P. Gosse, “Ion Injection in Hydrocarbons”, Journal of Electrostatics, Vol. 7, pp. 205-225, 1979.

[11] U. Gäfvert, O. Hjortstam, Y. Serdyuk, C. Törnkvist and L. Walfridsson, “Modeling and Measurement of Electric Fields in Composite Oil/cellulose Insulation”, Annual Report Conference on Electrical Insulation and Dielectric Phenomena, pp. 154-157, 2006.

[12] D.K .Ramesh, “Measurement Techniques for identifying polarity of Ion injection in transformer oil”, Master Thesis in Department of Materials and Manufacturing Technology, Chalmers University of Technology, 2012.

[13] M. S. Zadeh, “Measurement of ion mobility in dielectric liquids”, Master Thesis in Department of Materials and Manufacturing Technology, Chalmers University of Technology, Report No. 66/2011.